Isoporous Micro/Nanoengineered Membranes

Majid Ebrahimi Warkiani,[†,‡,*] Ali Asgar S. Bhagat,[§] Bee Luan Khoo,[⊥] Jongyoon Han,[†,∥] Chwee Teck Lim,[†,⊥,¶] Hai Qing Gong,[‡] and Anthony Gordon Fane[#]

[†]BioSystems and Micromechanics (BioSyM) IRG, Singapore-MIT Alliance for Research and Technology (SMART) Centre, Singapore 138602, [‡]Department of Mechanical and Aerospace Engineering, Nanyang Technological University, Singapore 639798, [§]Clearbridge Biomedics Pte Ltd., Singapore 139964, [⊥]Mechanobiology Institute, National University of Singapore, Singapore 117411, [∥]Department of Electrical Engineering and Computer Science, Department of Biological Engineering, Massachusetts Institute of Technology, Cambridge, Massachusetts 02139, United States, [¶]Department of Bioengineering, National University of Singapore, Singapore 117576, and [#]Department of Civil and Environmental Engineering, Nanyang Technological University, Singapore 639798

ABSTRACT Isoporous membranes are versatile structures with numerous potential and realized applications in various fields of science such as micro/nanofiltration, cell separation and harvesting, controlled drug delivery, optics, gas separation, and chromatography. Recent advances in micro/nanofabrication techniques and material synthesis provide novel methods toward controlling the detailed microstructure of membrane materials, allowing fabrication of membranes with well-defined pore size and shape. This review summarizes the current state-of-the-art for isoporous membrane fabrication using different techniques, including microfabrication, anodization, and advanced material synthesis. Various applications of isoporous membranes, such as protein filtration, pathogen isolation, cell harvesting, biosensing, and drug delivery, are also presented.

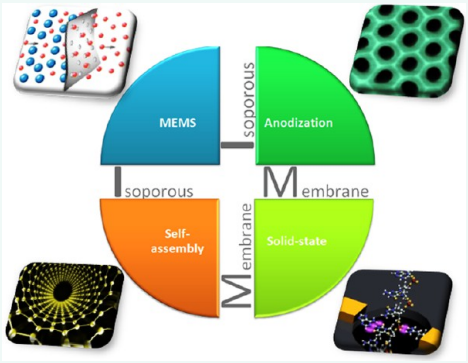

KEYWORDS: MEMS · nanotechnology · membrane · self-assembly · anodization · microfluidics · solid state · microfiltration · polymer · drug delivery · isoporous

Membranes with ordered pores (for consistency, we will use the term isoporous micro/nanoengineered membranes to refer to all micro/macroporous materials with the same pore size and shape which are parallel to each other) are ideal for various applications, from being barriers for selective transport and separation of chemical/biological species[1−3] to serving as stencils for micropatterning[4,5] and synthesis of nanostructures.[6] They can also serve as membranes for use in controlled, long-term, protein and drug delivery devices.[7,8] In addition, many biological processes occur at the micro- to nanoscale. Hence, the technology of isoporous membranes with hydrophilic pore environments is ideal for specific biological applications, such as biosensing and enzyme immobilization.[9−11] Purification of water is another avenue that has seen significant improvements in separation efficacy by the incorporation of isoporous micro/nanoengineered membranes.[12,13] The key characteristics of isoporous membranes, such as pore size, membrane area, morphology, biocompatibility, and thickness, can be tuned precisely as a function of the targeted applications and separation operations. Some of these applications with specific requirement for the membrane are summarized schematically in Figure 1.

Commercially available membranes (*e.g.*, cellulose acetate, glass fiber, and polytetrafluoroethylene (PTFE) filters) made with organic or inorganic materials present a random network of pores with a wide distribution of pore sizes. They normally have a tortuous microstructure, which makes it difficult to clean for reuse. Furthermore, they usually have a huge flow resistance due to the wide pore size distribution and membrane thickness, which in general compromises their performance, separation capability, and throughput. Among available commercial membranes, one of the most successful attempts to produce the ideal membrane (isoporous) is the track-etched membrane. For the production of track-etched membranes, dense polymeric films such as polycarbonate (PC), polyimide (PI), and polystyrene (PS) are randomly exposed to a high-energy ion bombardment.[2] This bombardment causes

* Address correspondence to majid@smart.mit.edu.

Received for review December 5, 2012 and accepted February 26, 2013.

Published online February 26, 2013
10.1021/nn305616k

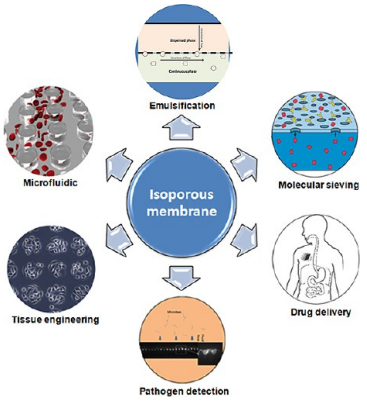

Figure 1. Illustration listing the various applications of the isoporous micro/nanoengineered membrane. The types of applications can be classified into various categories (not exhaustive). Emulsification: Membrane devices are of particular importance at generating precise drop-sized microemulsions or nanoemulsions. Isoporous membranes can improve this technique, with their flatness and pore uniformity, to achieve reduced coefficient of variations (COV) (below 10%) at a lower energy input,[2,26] as compared to conventional membranes (*e.g.*, microporous glass). Van Rijn *et al.* demonstrated the use of isoporous membranes for emulsification in 2004.[27] They employed silicon nitride membranes with extremely precise pore size ranging from 1 to 10 μm for this purpose. Molecular sieving: Separation of biomolecules using porous gel structures either by gel filtration or by gel electrophoresis has been used widely in various biological processes. Isoporous membranes have gained a considerable interest over the past decades for filtration of molecules based on size, shape, and interaction due to their ease of use and fast processing time.[3] For example, Fu *et al.*[28] fabricated a two-dimensional anisotropic filter array using interference lithography for high-resolution separation of DNA strands under a short time lapse *via* Ogston sieving mechanism. Drug delivery: Targeted drug delivery systems have been developed to deliver a certain amount of a therapeutic agent for a prolonged period of time to a specific organ while avoiding any damage to other healthy tissues.[8,29] Isoporous membranes can highly enhance control of dose administration profile due to their pore size tunability, narrow pore size distribution, and ability for selective functionalization. For instance, recent work by Yang *et al.*[30] illustrates how isoporous membranes made from block copolymers (with 10 nm pore size) can be employed in controlled protein delivery devices efficiently. Pathogen detection: Fast detection and recovery of waterborne pathogens is extremely important to secure the hygiene of drinking water. Available commercial membranes cannot be used effectively for this purpose because they suffer from several drawbacks such as rough surface, tortuous pore path, and low pore density. High-throughput isoporous membranes (*i.e.*, 2.5 μm pore size) made from nickel using electroplating techniques have been employed recently for enrichments of minute quantities of C. parvum oocysts from large volume of water samples successfully.[31] Tissue engineering: Most cell processes *in vivo* are controlled by microenvironmental stimuli, which can be a combination of many factors such as extracellular matrices and neighboring cells. Recently, isoporous microengineered membranes have emerged as a promising platform to create complex topography structures to mimic three-dimensional microenvironments of cells for studying cell interactions and artificial organs *in vitro*.[4] Microfluidics: Several groups have reported optimizing membranes (*i.e.*, made from silicon or polymer) for blood filtration, to carry out molecular analysis or for the removal of leukocytes.[32] Layers of filters can also be constantly adhered together in a microfluidic device to allow sequential rapid removal of cells from blood with minimal clogging.[33] Recently, planar isoporous membranes (*i.e.*, 6−10 μm pore size) have also been suggested for the precise isolation of rare circulating tumor cells (CTCs) with a low leukocyte contamination from blood of cancer patients.[34]

VOCABULARY: membrane - a permeable or semipermeable, solid phase (polymer, inorganic, or metal), which can be employed as a barrier for selective transport and separation of chemical/biological species or can be utilized as a stencil for cell patterning and synthesis of nanostructures; **microfabrication** - a process used in the semiconductor industry for fabrication of miniaturized structures and systems with micrometer- or sub-micrometer-scale features; **microfluidics** - the science and technology of designing and manufacturing miniaturized devices and processes that deal with small volumes of fluid on the order of nanoliters or picoliters; **anodization** - an electrochemical process that changes the surface chemistry of the metal, *via* oxidation, to produce an anodic oxide layer; **block copolymer** - a polymer consisting of multiple blocks of the same monomer alternating in series with different monomer blocks, which are covalently connected

the formation of linear damaged tracks across the irradiated polymeric film. These tracks are then revealed into pores using a well-chosen wet chemical etching (acid or alkaline solution).[2] The diameter of the pores is determined by the etch time. The pores that are being formed are cylindrical channels; however, the inherent random nature of the heavy ions during bombardment precludes the formation of well-ordered pores. Furthermore, these membranes normally produced with extremely low porosity (5−15%)[14] due to the fact that the chance for an overlap between two pores increases with the porosity. Even so, track-etched membranes have a low pore density with randomly distributed pores; they have been used widely as a template (so-called template synthesis method) for fabrication of various nanomaterials such as nanotubes,[15,16] nanoparticles,[17] and nanowires.[18] Recently, researchers have also shown that, by controlling the temperature and amount of EtOH (ethanol) in alkaline etching solution, track-etched membranes with conically shaped pores can also be produced.[19] These membranes can eventually be used for synthesis of conically shaped structures for a variety of industrial applications such as field-emission devices,[20] resistive pulse sensors,[21] drug delivery,[22] and electrochemical supercapacitors.[23] Another good example of commercially available isoporous membrane is the anodized aluminum oxide (AAO) membrane, which will be discussed in greater detail later.

Separation is a major cost component of most chemical, biological, pharmaceutical, and petrochemical processes. Advances in micro/nanofiltration require exploration of new technologies that yield highly permeable membranes characterized by high mechanical stability, adequate durability, and great selectivity. Recent advancements in the field of micro/nanofabrication have enabled high-throughput sample processing and inexpensive fabrication of

TABLE 1

Fabrication methods	Types of materials	Pore size	Density	Morphology	Applications	Advantages & disadvantages
MEMS (*e.g.*, Silicon micro-machining, Electroplating, Hot-embossing, Micro-molding)	Organic/Inorganic (*e.g.*, Silicon, SiO_2,Si_3N_4, Glass, SU8, PC, PMMA, Parylene, Nickel & Steel)	5 nm-1000 μm	10^6-10^{10} pore/cm^2	Any shape (*e.g.*, Cylindrical, Conical & Rectangular)	Ultrafiltration Photonics Tissue engineering Microfluidics Chromatography Biosensors Molecular sieving Drug delivery	Excellent mechanical stability Chemical inertness Biocompatible Expensive Versatile material Good for mass production High throughput
Anodization	Inorganic (*e.g.*, Aluminum, Silicon, Titanium &Magnesium)	5 nm-10 μm	10^9-10^{10} pore/cm^2	Cylindrical	Drug delivery Photonics Molecular sieving Nano-patterning Chromatography	Good mechanical stability Chemical inertness Biocompatible Relatively expensive Limited material choice Low throughput
Solid-state	Inorganic (*e.g.*, Silicon, SiO_2&Si_3N_4)	Down to 2 nm	N.A	Cylindrical&Conical	DNA& protein filtration Drug delivery Biosensors Biomimetic	Good mechanical stability Chemical inertness Biocompatible Expensive Limited to the Si_3N_4&SiO_2
Block-copolymers & self-assembly	Organic (*e.g.*, PMMA, PS, PVP, PLA,CNTs& PI)	0.7 nm-1000 nm	10^{10} pore/cm^2	Cylindrical	Ultrafiltration Nano-lithography Drug delivery	Poor mechanical stability Chemical inertness Biocompatible Expensive Difficult for mass production High throughput

SiO_2: Silicon oxide; Si_3N_4: Silicon nitride; PC: Polycarbonate; PMMA: Poly(methyl methacrylate); PS: Polystyrene; PVP: Poly(vinylpyrrolidone); PLA: Poly(lactic acid); PI: Polyimide; CNTs: Carbon nanotubes.

membranes, thus giving rise to potential applications in both micro- and macroscale processes.[24] However, transition to commercial success requires an economical process with precise "control over device" performance as well as scalability of the fabrication process.[25]

This review aims to introduce the various techniques developed to fabricate well-ordered isoporous membranes with micrometer and nanometer dimensions. These methodologies are classified to four different categories, including MEMS (microelectromechanical systems), anodization, solid-state nanopore, and block copolymers (Table 1). In lieu of this classification, detailed fabrication procedures for these methodologies are outlined, including material considerations. Characterization of each fabrication method in terms of their strengths and limitations is provided. Finally, various applications demonstrated using these membranes, including protein and cell filtration, pathogen isolation, biosensing, and drug delivery, are also cited. The objective of this review is to familiarize the reader with the burgeoning field of isoporous membranes, thereby empowering them to select the best fabrication methodology for their specific application. The readers are, however, encouraged to refer to the original papers for comprehensive details.

Isoporous Membranes Fabricated Using MEMS Technologies. *Inorganic Membranes.* In this section, we will present an overview of the existing methodologies employed to fabricate inorganic isoporous membranes and highlight some novel applications. MEMS, a technology which is used in the semiconductor industry for fabrication of integrated circuits, has been the workhorse behind the explosive growth of many industries such as aerospace, pharmaceutical, and automotive.[35,36] Micro/nanofabrication techniques can provide unprecedented control over feature size and geometry in a scalable manufacturing process. Patterning of micrometer-size features in metal foils using chemical etching (*i.e.*, wet etching normally using ferric chloride ($FeCl_3$)) emerged in the 20th century when the first photosensitive resists became available.[2,37,38] At present, photochemical etching is employed for the production of miniaturized metallic structures such as stencils, inject nozzle plates, springs, and sieves for numerous industries such as food, aviation, medical, and microelectronics.[2,39] However, the minimum feature size (*i.e.*, perforation diameter) is often limited by the material thickness.[40]

To overcome this limitation, Matsunaga's group produced uniform microcavities inside a thin steel film using direct laser drilling (so-called SUS micromesh) for isolation and detection of waterborne pathogens (*i.e.*, *Cryptosporidium* oocysts).[41] The trapped cells were visualized and counted on the micromesh using fluorescent microscopy. In a recent study, Warkiani *et al.*[31] fabricated high-flux isoporous membranes with an identical pore size and integrated back-support using multilevel lithography and nickel electroplating techniques, as shown schematically in Figure 2A. In this process, they initially produced micropatterns (or micropillars) on a photosensitive resist such as AZ9260 using conventional mask lithography and then employed electroplating to deposit nickel between photoresist features.

Electroplating offers the advantage of controlling the membrane thickness by varying the time and current. The resulting membranes using this technique

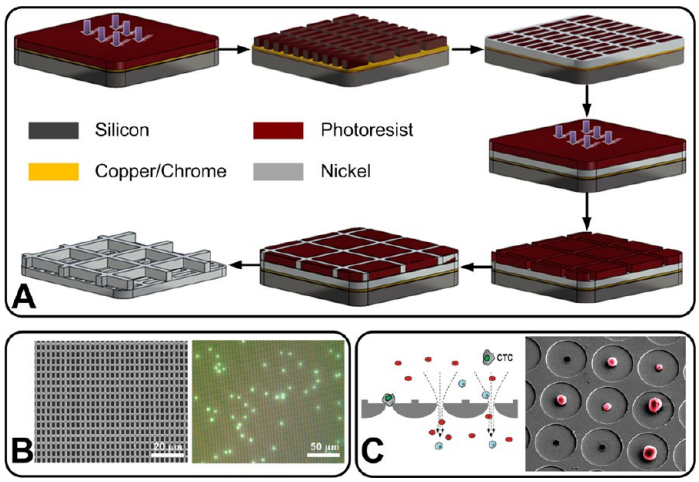

Figure 2. (A) Schematic illustration of the fabrication process of an isoporous metallic membrane by nickel electroforming. The process starts with deposition of a seed layer (Cr/Cu) on a Si substrate followed by spin-coating of a thick layer of AZ9260 photoresist on top and subsequent UV exposure through a quartz mask with rectangular-shaped features. After nickel is electroplated between the photoresist pillars, a second layer of AZ9260 photoresist is spin-coated again and exposed through a plastic mask with square-shaped features. Second electroplating of nickel between photoresist features is performed, and finally, the isoporous membrane with integrated back-support is achieved by dissolving the photoresist and seed layer in acetone and Cu etchant, respectively. Reprinted with permission from ref 31. Copyright 2012 Springer Science. (B) (Left) SEM image of an isoporous membrane with slotted pores. (Right) Fluorescence microscopic image of the membrane surfaces after filtration of Cryptosporidium oocysts. The slotted pores are 9 × 2.5 μm in size, with a 4 μm pitch. (C) (Left) Schematic image of CTC recovery using the size selective microcavity array. (Right) SEM image of MCF-7 cells trapped on the microcavity array. The microcavities are 9 μm in size, with a 60 μm pitch. Reprinted from ref 42. Copyright 2010 American Chemical Society.

have a smooth surface with narrow pore size distribution and can be as big as a 12 in. wafer. Their long lifetime and ease of cleanability make them also ideal for large-scale applications where conventional filters have to be replaced very often, like in the beer industry. Efficient isolation and recovery (more than 90%) of microorganisms from a large volume of water samples has been reported by these authors using these membranes. Figure 2B also shows a SEM and optical images of a metallic membrane with trapped cells on the membrane surface. Similarly fabricated metallic isoporous membrane has been used also by Hosokawa *et al.*[42] for efficient and rapid detection of circulating tumor cells (CTCs) from whole blood. They could successfully separate tumor cells from blood on the basis of differences in the size and deformability between tumor and hematologic cells for subsequent fluorescent microcopy (Figure 2C).

Considerable efforts have been devoted to the development of inorganic isoporous silicon (and silicon nitride (Si_3N_4)) membranes using standard silicon micromachining techniques such as photolithography, thin film deposition, and selective etching. The main features that make this material of interest are its mechanical properties, chemical inertness, high-temperature resistance, and biocompatibility.[43] Stemme and Kittilsland[44,45] were perhaps the first group who employed micromachining of silicon to fabricate isoporous membranes with very small pore sizes down to 50 nm for gas and liquid separation. They successfully combined conventional mask lithography and anisotropic silicon etching to pattern well-defined pores with uniform path length. This approach was further developed extensively by Ferrari and colleagues.[46−48] They employed top-down microfabrication methods to fabricate isoporous membranes consisting of arrays of parallel rectangular channels with pore size down to 7 nm.[49] Their proposed method comprised two basic steps: (1) surface micromachining of nanochannels in a thin film on the top of a silicon wafer using silicon dioxide as a sacrificial layer (*i.e.*, the thickness of the sacrificial oxide layer defines the nominal pore size in the final membrane); and (2) forming the final isoporous membrane by back-side etching of bulk silicon underneath the thin film structure.[49] The group successfully adopted these micromachined membranes to demonstrate applications such as immunoisolation and bioseparation (Figure 3A).[50−52] In a recent attempt, Roy *et al.*[53] employed sacrificial oxide etching for fabrication of high-performance microporous membranes in polysilicon to investigate its feasibility as an implantable bioartificial kidney. Their preliminary hemofiltration results using these membranes revealed a constant flux and consistent molecular selectivity for a period of 72 h.

Apart from silicon, silicon nitride (Si_3N_4) has been widely used to fabricate isoporous membranes. The first silicon nitride (Si_3N_4) membrane with precise pore dimensions was developed by Ogura *et al.*[54,55] in 1991 to investigate the deformability of individual red blood cells (RBCs) by simulating the passage of RBCs through capillaries. Afterward, Kuiper and co-workers at the University of Twente devoted comprehensive investigations on the development of silicon nitride membranes for various applications such as protein filtration and blood fractionation.[56−60] Figure 3B

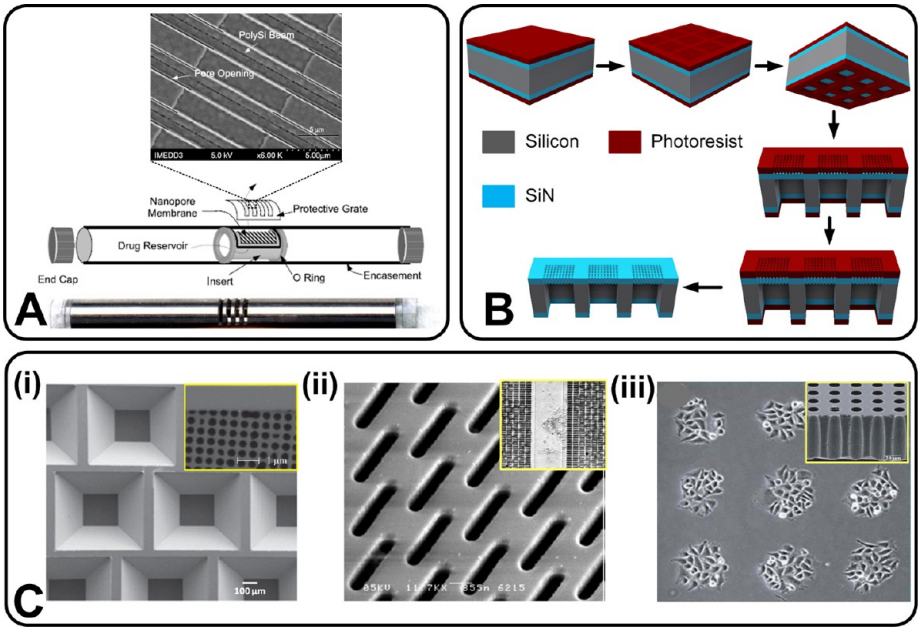

Figure 3. (A) (Top) SEM image of a nanopore membrane with 50 nm pores separated by silicon and polysilicon material. (Center) Drawing illustrating key features of the implant device fitted with nanopore membrane. (Bottom) Photograph of prototype implant device. Reprinted with permission from ref 49. Copyright 2005 Elsevier. (B) Fabrication process of a silicon nitride microsieve by standard mask lithography. The process begins with deposition of 1 μm thick LPCVD low-stress SiN deposition on a Si substrate followed by spin-coating of a thin layer of photoresist on both sides and subsequent contact mask lithography to define the desired pattern on both sides. Then using dry etching (RIE), the pattern of the photoresist is transferred into SiN from the top side, while KOH etching of the bulk Si from the back-side opens the windows for filtration. The final membrane can be achieved by removal of photoresist in the acetone bath. Redesigned from 61. (C) (i) SEM image of a silicon nitride membrane with circular pore shapes. The left image shows the membrane from the back-side with silicon bars, and close-up images show the membrane surface and cross section. Reprinted with permission from 62. Copyright 2012 Institute of Physics. (ii) SEM micrograph of an isoporous membrane with slotted perforations. The inset shows the membrane surface after filtration of lager beer. Reprinted with permission from 63. Copyright 2001 Elsevier. (iii) Phase contrast microscopy image of HeLa cells patterned with an isoporous membrane (*i.e.*, a stencil) shown in the inset. Reprinted with permission from ref 64. Copyright 2011 The Royal Society of Chemistry.

schematically shows the fabrication process for the realization of thin silicon nitride membranes.

In this process, a low-stress silicon nitride film is deposited on a silicon substrate (*i.e.*, both sides) by low-pressure chemical vapor deposition (LPCVD).[57] Then, a thin photosensitive layer (*i.e.*, photoresist) is spin-coated and patterned on the nitride film to serve as a masking layer during the subsequent etching step (typically using reactive ion etching (RIE)). In order to release the membrane, the silicon substrate is anisotropically etched from the back-side using a potassium hydroxide (KOH) solution.[57] Figure 3C-i shows the SEM image of a silicon nitride microsieve obtained with this technique. The pore size using conventional UV lithography is typically limited to >1 μm, due to the wavelength of light and the reduction lens system.[65] To overcome this, they employed a laser interference lithography technique to transfer the desired pattern into the silicon nitride thin layer. Over the past decade, various techniques such as block-copolymer-assisted lithography,[66,67] nanosphere lithography,[68] electron-beam (E-beam) lithography,[52,69,70] deep-ultraviolet (DUV) lithography,[71] track-etching,[72] and thermal-imprint lithography[62] have been employed by different researchers to define submicrometer holes (down to 10 nm) in a thin nitride film. A considerable number of applications have emerged using these membranes recently. For instance, Kuiper and his colleagues[63] used them as a microsieve for high-throughput yeast cell filtration from lager beer (Figure 3C-ii). They could successfully achieve a high permeate flux of up to 4000 l/m^{2}h without any significant increase in transmembrane pressure (TMP) during the course of the experiment. The same group has employed these membranes for depletion of white blood cell (WBCs) from red blood cells (RBCs) with an efficiency of 99%.[56] In another study, they successfully incorporated a thin layer of palladium (as a gas-permeable layer) on top of microsieve apertures for hydrogen separation.[73,74] More recently, their group also demonstrated the application of high porosity microsieves for efficient emulsification of vegetable oil in water.[75] They have shown that emulsification with these membranes can lead to stable emulsions with a low droplet span. These membranes have also been used for filtration and detection of airborne pathogens as well as *E. coli* from drinking water.[76−79] In an interesting study, Harris and Shuler[52] utilized silicon nitride membranes as a platform for culturing endothelial cells (*e.g.*, BAEC, HUVEC) to model the blood−brain barrier (BBB).

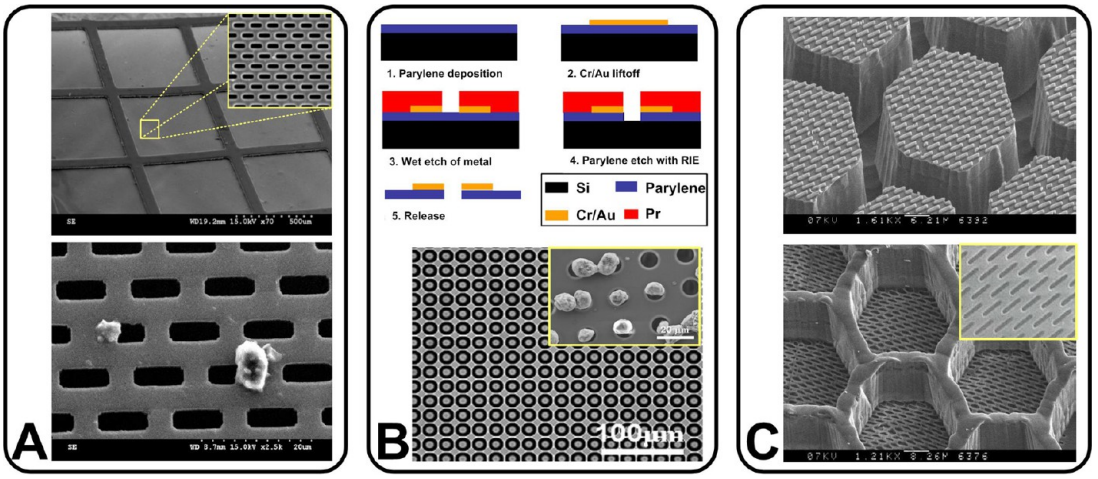

Figure 4. (A) (Top) SEM image of a microfilter with an integrated support mesh made from SU-8. The inset shows the perforated membrane with slotted pores. (Bottom) SEM image of a membrane with trapped C. parvum oocysts between the pores. Reprinted with permission from ref 87. Copyright 2011 Institute of Physics. (B) (Top) Schematic of fabrication process for an isoporous membrane with integrated electrodes for cell electrolysis. (Bottom) SEM image of a polymeric membrane with circular pores made from parylene. The inset shows the captured CTCs within the membrane pores. Reprinted with permission from ref 97. Copyright 2007 Elsevier. (C) (Top) SEM micrograph of a Si mold made with MEMS techniques for making an isoporous membrane with slotted perforations using the imprinting approach. (Bottom) SEM image of a through-hole membrane with back-support. The inset shows the membrane surface. Reprinted with permission from ref 2. Copyright 2004 Elsevier.

Their experimental results with this model revealed that endothelial and astrocyte cocultures can be maintained by using a collagen-covered membrane for around 2 weeks. Furthermore, silicon nitride membranes with submicrometer apertures have also been used as miniature shadow masks or nanostencils for resistless patterning of mesoscopic structures.[71]

Similarly, single-crystalline silicon can also be used as a membrane material for fabrication of high aspect ratio isoporous membranes. Using the advantages of UV-nanoimprint lithography and deep reactive ion etching (DRIE), high aspect ratio (10:1 or greater) membranes have been fabricated with silicon-on-isolator wafers (SOI).[61,80,81] In a recent study, Wu *et al.*[64] employed a silicon isoporous membrane as a reusable stencil for micropatterning of cells (Figure 3C-iii). For energy applications, micromachined silicon membranes have also been utilized successfully in development of novel polymer electrolyte membrane (PEM) fuel cells.[82]

Micromachined isoporous membranes, made from silicon and silicon nitride, are particularly attractive due to the excellent control over feature size and their high mechanical strengths aiding membrane handling.[80,83] In addition, such membranes have an extremely small flow resistance due to their thickness being smaller than the pore size and are relatively insensitive to particulate fouling, making them ideal for various industrial applications.[57] These membranes can be made by standard microfabrication techniques on the silicon wafers up to 12 in. However, they must be produced in a cleanroom environment requiring expensive machinery. Therefore, most of their applications are in small-scale systems where separations of precious samples such as stem cells or proteins are required.

Organic Membranes. Inorganic isoporous membranes made from silicon-based materials are durable filters with exceptional chemical inertness. For applications where disposable filters are preferred, the use of high-quality micromachined silicon membranes may not always be economically feasible.[83] Alternatively, low-cost isoporous membranes fabricated in polymers are becoming increasingly popular. Apart from cost, the physical and chemical properties of polymeric membranes can be easily tuned by selecting appropriate materials and surface modification.[84] Polymeric isoporous membranes can be fabricated by direct photoetching (development) of a photosensitive polymeric film (*i.e.*, normally negative-based photoresist) using the contact mask lithography. Brouker *et al.*[85] employed this approach for fabrication of a macroporous polymeric membrane using polyimide for biomedical applications. Polyimide is a strong engineering polymer with exceptional thermal stability (>500 °C) and chemical inertness as well as mechanical robustness, having half the tensile strength of steel.[86] In their proposed method, a polyimide layer, which was initially spin-coated on a substrate, was directly exposed to UV light through a photomask and subsequently developed using a suitable developer. This procedure can be repeated to pattern several layers of polyimide to form a multilayer structure suitable for filtration. The polyimide assembly is then detached from the substrate by dissolving the supporting silicon wafer inside a KOH solution bath. Recently, Warkiani *et al.*[87,88] also reported a low-cost and rapid method for fabrication of multilayer polymeric membranes with

hierarchical structures. The microfabricated filters are made of several layers of SU-8 photoresist using multiple coating and exposure steps with a single final developing process (Figure 4A). The group successfully applied these isoporous filters for the efficient isolation and recovery of *C. parvum* oocysts from tap water. Alternative exposure methods including wafer stepping or laser interference lithography,[83,89−91] atom-beam lithography,[92] and nanoimprint lithography[93] have also been used by other groups to fabricate free-standing polymeric membranes with well-controlled pore sizes and geometries. Aperture array lithography has been utilized for fabrication of polymeric isoporous membranes.[94] In this method, ion beam lithography (*i.e.*, used for patterning of a thin photoresist film) and reactive ion etching (*i.e.*, used for transferring the pattern to a thick polymeric film beneath the photoresist layer) techniques have been combined to produce membranes with a homogeneous pore diameter on the scale of hundreds of nanometers. Using this technique, Zheng *et al.* developed novel polymeric membranes with various pore shapes (circular and slotted) made from parylene for isolation of circulating tumor cells (CTCs) from blood.[95,96] In one of their designs, they successfully integrated electrodes on the membranes for *in situ* lysis of trapped cells and subsequent genomic analysis (Figure 4B).[97] PDMS through-hole membranes with various pore size and shape were also produced recently by other researchers using the aforementioned technique for microfluidic applications.[98,99]

Micromolding technique using an elastomeric/solid replica of the desired features has also been utilized for fabrication of polymeric isoporous membranes. Whiteside's group at Harvard developed a novel method for fabrication of free-standing membranes by micromolding of sol−gel precursors.[100] More recently, polymeric isoporous membranes were produced by phase separation micromolding[84,101] and dissolving mold techniques.[12,102] In phase separation micromolding, sieve formation relies on phase separation of a polymer solution which is cast on an inorganic master mold such as silicon. Intrinsic shrinkage, which occurs during the phase separation process, helps to release the sieve from the mold. In the dissolving mold technique, dissolution of a polymeric pillar mold makes perforations in the deposited polymer. Using a micropatterned Si wafer prepared by micromachining techniques, polymeric membranes with precisely microscaled pore size have also been fabricated by a hot-embossing method.[2,83] In this approach, a thermal plastic polymer such as polycarbonate (PC), which is heated above the glass temperature, is pressed against the Si mold (*i.e.*, master mold). After conforming to the Si mold, the polymer is cooled to room temperature and subsequently released from the master mold (Figure 4C). These membranes can be produced on the large scale (hundreds of square meters) using roll-to-roll printing by employing master molds made from a microstructured nickel foil which can easily be wrapped around a drum for continuous production.[2]

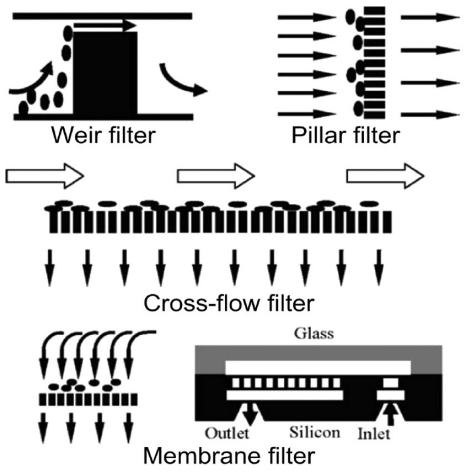

Figure 5. Planar microfluidics membranes. Schematic illustrating commonly used isoporous filtration features patterned in microfluidics channels. The gap between the features can be tuned to vary the pore size and density depending on the application. Reprinted with permission from ref 112. Copyright 2008 Springer Science + Business Media.

Similar to the metallic membranes, direct drilling of micron sized holes inside polymeric films using a laser has been investigated by many groups. For example, Atkin *et al.*[103] employed laser machining for direct patterning of microholes inside a 12 μm polyethylene terephthalate (PET) film. They could successfully use this membrane for blood filtration and subsequent DNA extraction for molecular analysis. In a follow-up study, Saxena and co-workers[104] fabricated isoporous polymeric membranes with pore size down to 12 μm by laser drilling of a polyimide film using a KrF-based excimer laser. They employed these membranes as a platform for investigating pressure drop in the microcapillaries by measuring the air flow rates. The advantage of laser drilling is that isoporous membranes with large surface area can be manufactured at low cost in a broad range of materials; however, some challenges such as pore size variation in the front and back of the membrane (angled walls) as well as debris due to laser ablation are associated with this method.

Planar Isoporous Membranes for Microfluidic Devices. Microfluidics is an interdisciplinary field at the interface of chemistry, engineering, and biology[105] which has been used extensively for various applications such as separation,[106] DNA and proteins synthesis,[107] and molecular assays[107] due to advantages associated with miniaturization, integration, improved sterility, and faster sample processing times.[108,109] Many microfluidic chips have been developed with pillars or weirs patterned within them for the separation of cells and other biomolecules. As the spacing between these pillars and weirs is

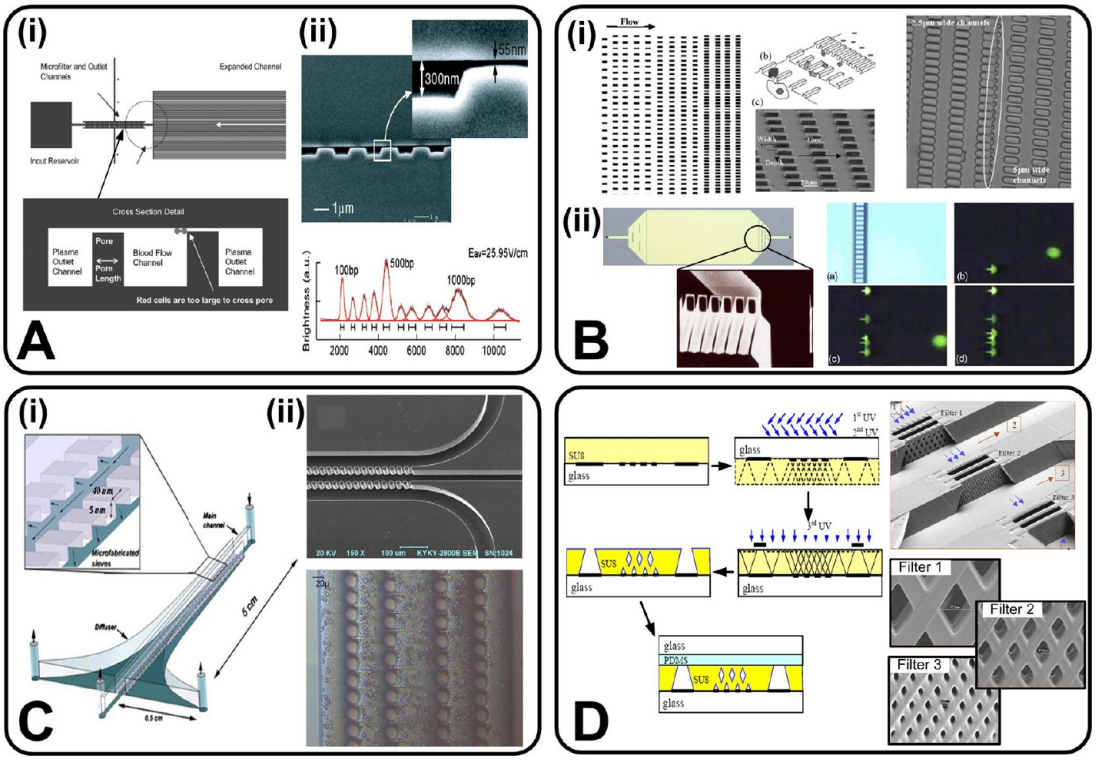

Figure 6. (A) (i) Schematic presenting the device design of isoporous weir filters for the isolation of plasma from whole blood. Blood is introduced through the center channel, and the weirs impede the flow of cells into the side while allowing plasma to diffuse across. Reprinted with permission from ref 111. Copyright 2005 Royal Society of Chemistry. (ii) (Top) SEM images of nanofilter weirs for molecular sieving of DNA and proteins. The image shows alternating deep (300 nm) and shallow (55 nm) regions patterned in silicon. (Bottom) Electropherograms showing the separation of a 100 bp DNA ladder in the nanofilter. Reproduced with permission from ref 116. Copyright 2005 The American Physical Society. (B) (i) (Left) Schematic of a micropillar array with successively decreasing gap sizes for size- and deformability-based cell separation. (Right) Microscope image showing goose red blood cells retained at the start of the 2.5 μm gap micropillar array. Reprinted with permission from ref 122. Copyright 2007 Elsevier. (ii) (Left) Schematic and scanning electron micrograph of a micropillar array for white blood cells isolation from blood. (Right) Time-lapse images of white blood cells trapped at the micropillar array. The white blood cells are stained with fluorescent nuclear dye for enhanced viewing. Reprinted with permission from ref 122. Copyright 2007 Elsevier. (C) (i) Schematic illustration of a cross-flow filtration microchannel consisting of weirs for the isolation of rat myocytes from myocardium tissue. The larger myocytes are retained in the center channel, while the nonmyocyte cells can pass through the weirs into the side channels. Reprinted with permission from ref 125. Copyright 2006 Springer Science + Business Media. (ii) (Top) Scanning electron micrograph of a micropillar array for the cross-flow filtration of white blood cells from whole blood. (Bottom) Microscope image of a multilevel cross-flow filtration for the fractionation of white blood cells, red blood cells, and plasma from whole blood. Whole blood is pumped through the center channel, with the white blood cells being retained at the first pillar array and the red blood cells at the next pillar array with pure plasma collected at the side channels. Reproduced with permission from ref 126. Copyright 2008 Elsevier. (D) (Left) Schematic illustrating the fabrication process of patterning vertical screen filters in SU-8 photoresist using multiple exposure interference lithography. (Right) Integrated filters with decreasing pore diameter patterned within a microfluidic channel for multiple particle separation. The pore diameter of filters 1−3 is measured to be 57.3, 27.3, and 10.0 μm, respectively. Reproduced with permission from ref 127. Copyright 2003 IEEE.

constant, such devices can also be considered as isoporous filters. In this section, we review standard microfabrication techniques employed to realize these features and present examples of integrated isoporous filters for versatile application in fluidics systems.

Microfabrication techniques have facilitated the development of microfluidic systems with very accurate size control and structure uniformity. The fluidic channels (so-called microchannels) are commonly etched or molded into materials such as glass, silicon, or polymer (*e.g.*, COC, PDMS, PMMA) using either deep reactive ion etching (DRIE) or other microfabrication techniques. Microfluidic chips fabricated from silicon and glass are emerging as an important new type of analytical device for a wide range of applications, including size-based separation of biological components. A complete microfluidic system for size-exclusion assays normally consists of sieving structures, supply channels, and feed-through components to deliver the sample. In the most common approach, an initial pattern is normally defined on a silicon/glass wafer by means of lithography. After definition of channels and features, wet (using chemicals such as KOH or TMAH) or dry etching (using RIE or DRIE) of silicon/glass is performed with an optimized recipe to etch the features and the microchannels simultaneously. Lastly, the microfluidic device is completed by bonding a flat surface (a glass slide as an example) to the

micropatterned layer using either adhesive or anodic bonding to make the final assembly. Figure 5 illustrates the distinct designs, weirs, pillars, cross-flow, and membrane which have been widely used as sieving structures inside the microfluidic devices.[110,111] The weir-type design includes an array of individual barriers (resembling a dam) obstructing the flow path for trapping particles/cells of certain size while allowing smaller constituents to squeeze through the narrow slits located on top of the barrier. In other designs, this barrier can be altered with an array of well-ordered micropillars (or microposts) where the main flow is either perpendicular or tangential to the filters.

Wilding and co-workers[113] were the first group to introduce the use of a silicon micromachined isoporous filter for blood separation and other biological assays.[114] They designed a weir-type filter with a 3.5 μm gap between the silicon structure and a Pyrex top cover (*i.e.*, attached together using anodic bonding) for effective isolation of WBCs from RBCs. Similarly, Crowley and Pizziconi[111] demonstrated the separation of plasma from whole blood for clinical diagnostic applications using weirs (see Figure 6A-i). The device can effectively isolate nanoliter volumes of plasma from a single drop of blood. Similarly, isoporous planar membranes with comparable molecular dimensions have also been employed by researchers as an alternative to conventional approaches (*e.g.*, polymeric gels and electrophoresis) for separation and concentration of complex biomolecules such as DNA, RNA, and proteins. For instance, Austin and co-workers[115] used a biochip consisting of micrometer-sized pillars of silicon for electrophoresis of DNA. Furthermore, nanofluidic weirs acting as entropic traps have been developed for the separation of long DNA molecules (see Figure 6A-ii).[116,117] A broader discussion about artificial molecular filters and their fabrication methods can be found in various reviews on the subject.[28,118,119]

Pillars or posts with regular spacing between them have been widely used in microchannels for a wide range of applications. Complex processes such as cancer metastases (*i.e.*, extravasation and migration of primary tumor cells) have been mimicked *in vitro* by Chaw *et al.*[120] using a multistep microfluidic device with silicon micropillars. Matrigel was coated between the gap of pillars to model the basement membrane in the human body. In another study, Peh and his colleagues[121] used silicon micropillars to make a filter-based biochip for separation and detection of *C. parvum* oocysts and *Giardia lamblia*. Their design included a bypass region with slightly wide openings, acting as an alternative fluidic flow route to relieve pressure changes, and a fine region (1 μm pitch) for trapping the protozoa cells. Silicon microchips with well-defined micropillars have been used as a non-invasive method for isolation of fetal cells from maternal circulation (Figure 6B-i).[122] The device allows the enrichment of

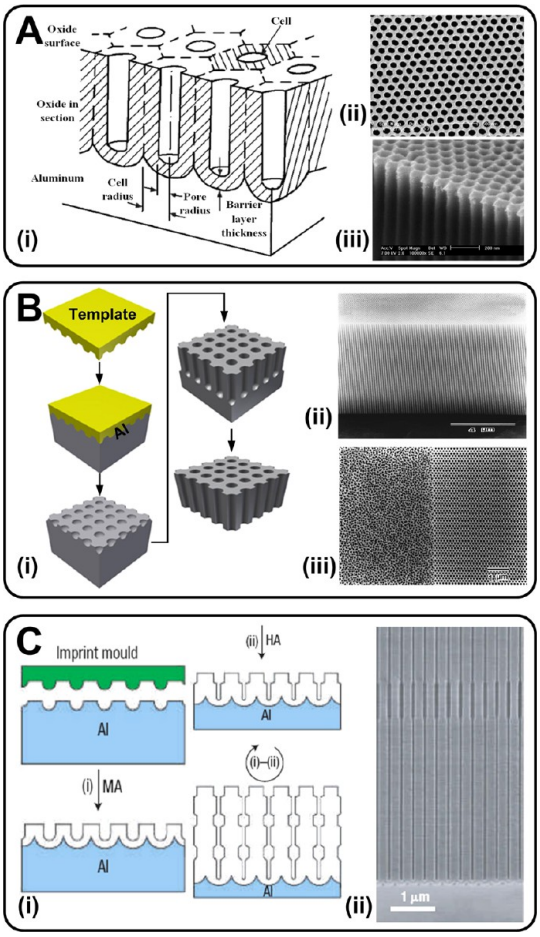

Figure 7. (A) (i) Schematic illustration of the a porous alumina template clearly revealing the hexagonal cells and the cylindrical pores. Reprinted with permission from ref 164. Copyright 1989 Macmillan Publishers Ltd. (ii,iii) Top view and cross-sectional view of porous alumina membranes with pore diameter and cell size of about 65 and 105 nm, respectively. Reprinted with permission from ref 165. Copyright 2007 Elsevier. (B) (i) Process flow for fabrication of an isoporous nanoporous membrane using anodization. The process starts with pretexturing of a thin aluminum film using a solid mold followed by anodization and growth of channel architecture in an appropriate solution. Following anodization, the back-side aluminum film and the aluminum oxide barrier film are removed by a mercury chloride solution to form the through-hole membrane. (ii) Cross-sectional view of the channel array of an anodic alumina membrane. (iii) SEM micrograph of an anodized membrane with (right) and without (left) pretexturing. Reproduced with permission from ref 154. Copyright 1997 American Institute of Physics. (C) (i) Illustration showing the fabrication of an isoporous alumina membrane with modulated pore diameters by a combination of MA and HA technique on a prepatterned aluminum film. (ii) SEM image showing the cross section of a high aspect ratio membrane (>1000) with uniform nanopores. Reprinted with permission from ref 151. Copyright 2006 Macmillan Publishers Ltd.

less deformable and larger fetal cells, which are retained within the microchannels. On-chip isolation and genomic analysis of WBCs from whole blood have also been demonstrated by Panaro *et al.*[123] using micromachined silicon microfluidic chips patterned with an array of silicon microposts (Figure 6B-ii). Similarly, CTCs, which are generally larger and stiffer than

blood constituents, have been isolated using a biochip comprising micropillar arrays with different gap sizes.[124]

Cross-flow filtration is a process whereby most of the fluid flows along a direction that is tangent to the membrane surface,[128] thus the process is less prone to fouling. In a detailed study, Ji *et al.*[112] investigated the isolation efficiency of four different types (*i.e.*, weir, pillar, cross-flow, and membrane filter) of planar microfilters for separation of WBCs from RBCs inside a silicon biochip. The critical dimension of all microfilters was fixed to 3.5 μm. Their results indicate that the cross-flow design has superior performance in terms of throughput (*i.e.*, whole blood handling capacity) and also isolation efficiency.[112,129] This has also been confirmed by others for the separation of blood components such as nucleated RBCs (nRBCs) from RBCs, too.[126,130] Murthy *et al.*[125] developed a device consisting of a middle channel connected to adjacent side channels by polymeric microposts to enrich neonatal rat myocardiac cells. The side channels increase in width in a flared shape along the length of the device to ensure a constant pressure delivery during filtration (Figure 6C-i). Similarly, Chen *et al.*[126] designed and fabricated cross-flow filtration-based microchannels consisting of pillars with isoporous spacing to isolate WBCs from blood. Their device achieved twice the efficiency of WBC isolation as compared to dead end membrane devices (see Figure 6C-ii).

In situ fabrication of polymeric isoporous membranes inside the microfluidic channels has been realized using advances in holographic and inclined lithographic techniques.[127,131] A hologram is usually reconstructed by the diffraction of light from a photosensitive film previously recorded with an interference pattern produced from coherent polarized light. Using this method, a triple sieving system with multiple inlet and outlet streams and three different mesh sizes of 57.3, 27.3, and 10 μm had been fabricated (Figure 6D) by Yoon *et al.*[127] for filtration of microparticles. The advantage of this approach is that the sealing to complete the channel is not of concern during manufacturing because the membrane is made of the same material as the microfluidic chip during lithography steps.[131]

Fabrication of isoporous planar filters for lab-on-chip devices is a straightforward process because it can be a part of the chip fabrication process. However, several issues including specificity and channel clogging have limited their large-scale use. These kinds of filters are normally produced for single use applications such as point-of-care devices; therefore, they must be manufactured on a large scale with relatively low cost.

Isoporous Membranes Fabricated by Anodization. Anodization is the process of oxidizing a chemical species by applying appropriate voltage of current in an electrolytic solution. The anodization of metals has intensively been utilized in industry for various applications, including the formation of electrically insulating layers, anticorrosion coatings, and decorative coloration of metal surfaces. During this electrochemical process, the surface of the metal will be covered by a nanoporous oxide layer. Oxide layers generated during anodization can be produced on various materials such as magnesium (Mg), aluminum (Al), silicon (Si), tantalum (Ta), titanium (Ti), tungsten (W), zinc (Zn), and zirconium (Zr).[132]

The growth of self-assembled porous oxide on aluminum metal templates by anodization has emerged as a growing area of interest in recent years.[133] Porous anodic aluminum oxide (AAO) membranes with honeycomb-like pore structure have garnered significant attention primarily being employed as a nanoporous template for development of various functional nanostructures, such as nanowires,[134−136] nanotubes,[137,138] nanodots,[139,140] optical devices,[141,142] and nanomaterial synthesis.[143,144] More recently, membranes with nanopore dimensions fabricated by anodization have found applications in the biomedical field as a size-selective sieve,[145,146] sensors, and drug delivery platform.[21,147] In this section, we describe the fabrication of AAO membranes, due to the highly controllable pore diameter and cylindrical shape, and also discuss briefly other materials used for fabrication of membranes by the anodization process such as silicon.

A typical anodization process to fabricate porous alumina membranes (also commonly known as mild anodization (MA)) is carried out by placing a pure aluminum film (99.99% purity or higher) in an electrolyte solution and applying DC bias between the anode and cathode. In this case, the aluminum film acts as an anode, and a platinum mesh is popularly used as a cathode. When a neutral electrolyte is used, a self-ordered layer of aluminum oxide having hexagonal domains with pores is formed on the surface of the aluminum film.[148] When an acidic electrolyte is chosen (pH <4), such as sulfuric acid (H_2SO_4), phosphoric acid (H_3PO_4), or oxalic acid ($H_2C_2O_4$), this layer of aluminum oxide is locally dissolved by hydrogen ions in the presence of an electric field to form pores perpendicular to the surface of the aluminum film.[149,150] It should be noted that neighboring pore growth prevents growth in any other direction. The final structure ideally consists of a densely packed hexagonal array of ordered pores with uniform intervals (Figure 7A). The pore diameter can range from 4 to 200 nm with an interpore distance of 7−500 nm and porosity of 10^8−10^{12} pores/cm^2.[132] These characteristics of the membrane in this self-organized process can be controlled by the applied DC voltage as well as composition, concentration, and temperature of the electrolyte.[149] However, if the anodization process is carried out outside the self-ordering regimes, the degree of spatial ordering decreases significantly.[151] Following anodization,

the back-side aluminum film and the aluminum oxide barrier film can be removed by either etching in mercury chloride solution or electrochemical detachment using a pulsed voltage.[152,153] The final pore size can be further adjusted by post-etching treatment in a dilute phosphoric acid. During single-step anodization, the pores nucleate and develop randomly over the aluminum surface. As the anodizing time increases, the pore patterns continue to develop and become more ordered; however, obtaining a large defect-free area from this naturally ordering process is difficult and is limited to the size of several micrometers.[154] To solve this issue, Masuda and Fukuda[155] proposed a novel approach for precise control of the growth of the channel array over a large surface area using a pretextured aluminum film and subsequent mild anodization. In their proposed method (Figure 7B), shallow concave features that act as initiation sites for regular pore development during anodization were patterned on the Al film by mechanical imprinting using a solid mold. Subsequently, through-hole membranes were achieved by removing the aluminum substrate and barrier layer in a saturated $HgCl_2$ and phosphoric acid solution, respectively.[154,155]

The required mold for pretexturing (imprinting) can be fabricated by electron-beam (EB) lithography on a single-crystal SiC,[156,157] silicon nitride (Si_3N_4),[158] and using metals such as nickel.[159] In addition, pretexturing using a focused ion beam (FIB) apparatus[160] and an array of polystyrene particles has also been reported.[161,162] Using anodic porous alumina as a template, Masuda and co-workers also produced high aspect ratio (~150) polymeric[163] and metallic[156] membranes with channel density of 10^{10} cm^{-2}. The resulting membranes using this approach are extremely uniform with identical pore sizes, and all of the pores were perfectly placed parallel to each other. The physical geometry of the obtained polymeric/metallic membranes was in good agreement with those of anodic porous alumina templates, too.

A major limitation of mild anodization is the time required to fabricate these porous membranes. Depending on the length of the pores, the processing time can vary between 18 h and several days. In contrast, hard anodization (HA), which is normally carried out at much higher voltages by using sulfuric acid, results in the rapid growth of a thick porous oxide layer.[166] Recently, Lee *et al.*[151] combined MA with HA to fabricate perfectly ordered alumina membranes with aspect ratio larger than 1000 in a short period of time, as shown in Figure 7C-i (25−35 times faster than normal MA process). Figure 7C-ii shows the SEM image of a high aspect ratio alumina membrane with modulated pore diameter fabricated using this method.

Although AAO membranes are perhaps the most popular nanoporous material fabricated by anodization, macroporous silicon membranes with perfect cylindrical pores have also attracted increasing interest for a wide spectrum of potential applications including photonics[167] and solar and fuel cells.[168] These membranes are fabricated using electrochemical etching of silicon under appropriate conditions, resulting in the formation of a porous layer on the silicon substrate.[169] The initial domains for anodization (self-assembled hexagonal array in the case of aluminum) are patterned using conventional photolithography and subsequent alkaline etching. Similar to the aluminum anodization process, the silicon wafer was normally etched in hydrofluoric acid (HF) under appropriate anodic bias.[169] The pore diameter is a function of the electrochemical conditions used for their growth and the type (crystal plane orientation) and resistivity of the silicon substrate.[169] Lehmann *et al.*[170] successfully employed macroporous membranes with cylindrical pores as an optical short-pass filter for near- and mid-infrared spectral range. They have shown that, under vacuum condition, these filters can be functional all the way down to wavelengths on the order of a few nanometers. Membrane characteristics such as pore radius, pore density, and pore length can be altered to tune the frequency range. A comprehensive review of Si porous membranes and their applications was published by Foll *et al.*[171]

In recent years, there has been renewed interest in micro/macroporous membranes fabricated by anodization for use as templates in a variety of nanotechnology applications. For instance, Masuda and Satoh[139] have used this technique to produce a highly ordered gold nanodot array over a large area of Si substrate. Nanodot arrays of other materials such as Co, InAs, Fe, and Ni have also been deposited on various substrates using the same technique.[136,172] Figure 8A-i shows a SEM of hexagonally ordered InAs quantum dots fabricated using the AAO membrane.[140]

Martin's group has devoted great efforts for development of various nanostructures, such as nanoparticles and nanotubes for biomedical applications, including enzyme encapsulation, DNA transfection, biosensors, and drug delivery.[173−175] For example, using synthesized silica nanotubes, they have reported fabrication of smart nanophase extractors to remove molecules (*e.g.*, lipophilic) from aqueous solution.[16] Recently, they also demonstrated the production of biodegradable nanoparticles of the polysaccharide polymer chitosan using AAO membranes for drug delivery.[17] The application of AAO membranes in molecular filters has also been discussed elswhere by Martin *et al.*[176] Recent studies have shown that the synthesized nanowires can have a significant impact on the future development of new electronic devices. The magic properties of these tiny structures can significantly enhance the superconductivity[177,178] of some materials while improving the thermoelectric properties[179] of others. It has been reported that nanowires can boost the sensitivity of biosensors[180]

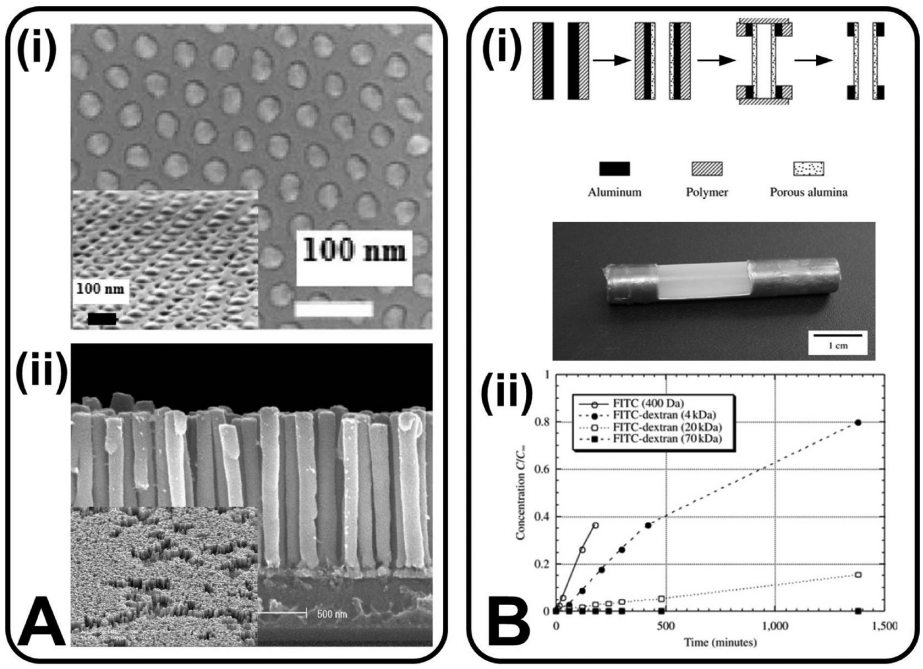

Figure 8. (A) (i) Scanning electron microscope (SEM) image of hexagonally ordered an InAs quantum dot array patterned using a AAO template. Reproduced with permission from ref 140. Copyright 2004 American Institute of Physics. (ii) Scanning electron micrographs of palladium nanowires standing freely after removal of the AAO template. (Inset) Large-area patterning of palladium wires using AAO membranes. Reprinted with permission from ref 136. Copyright 2006 Elsevier. (B) (i) Schematic illustrating the process steps to fabricate a tubular anodized aluminum oxide membrane for controlled drug delivery. Silicon is used to cap the two ends of the capsule filled with a drug solution. (ii) Plot showing the normalized release rates of molecules of varying weight through a AAO capsule with 55 nm pore diameter. As expected, smaller molecules are released at a much faster rate compared to larger molecules. Adapted with permission from ref 147. Copyright 2003 Kluwer Academic Publishers.

and e-nose sensors[181] and also improve the efficiency of plasmonic devices.[182] Figure 8A-ii shows cross-sectional SEM images of free-standing Pd nanowires. Due to the extremely high surface-to-volume ratio of alumina membranes, capsules fabricated of anodized aluminum have been demonstrated for controlled molecular filtration for drug delivery applications.[147] Gong and co-workers demonstrated the transport of FITC-conjugated dextran of varying molecular weight (and hence size) through nanoporous alumina as a function of time. Such membranes can be used as drug delivery carriers for long-term drug release *in vivo* (Figure 8B). Finally, as the primary application of any isoporous membrane is size-based separation, AAO membranes have also been used for size-based molecular separation. Yamaguchi *et al.*[145] recently presented an application of nanoporous alumina for the separation of protein molecules having >4 nm size from molecules with <2.4 nm diameter. However, an obvious concern of these membranes is the extremely low-throughput, limiting their application as a filtration method. Depending on the size of the biomolecule, extremely low fluxes of 2−20 nmol per hour are typical of these membranes.[147]

Solid-State Nanopores. In the past decade, nanometer-sized isoporous membranes have been fabricated using traditional silicon microfabrication methods developed in the microelectronics industry, so-called solid-state nanopores.[183] These membranes have been extensively used as nanosensors for the detection and characterization of biomolecules including DNA and proteins with single-molecule precision.[184−186] This has ultimately led to the application of these solid-state nanopores as an ultrafast DNA sequencing technique.[187,188] In this section, we will review the methodology employed to fabricate these nanopore membranes and introduce a few popular applications demonstrated to date. Although the field of solid-state nanopores is fairly nascent, it has already triggered an avalanche of developments in this area. Their importance is validated by detailed review articles published highlighting their significance and applications.[11,183,185,187−191]

As the name implies, these nanopore membranes are developed using standard solid-state fabrication techniques. The nanopores are typically fabricated in silicon nitride (Si_3N_4) or silicon oxide (SiO_2) membranes, as these have been extensively studied and used in the semiconductor industry for over five decades. The ability to deposit/grow stable 10−50 nm layers of Si_3N_4 and SiO_2 on silicon wafers makes them attractive starting material for solid-state nanopores. Typical fabrication of these nanopores begins with the growing of a thin Si_3N_4 or SiO_2 layer on a silicon substrate by either LPCVD or PECVD techniques. Following this, a micrometer-sized window is etched on the supporting silicon wafer to form free-standing nanometer thin membranes (Figure 9A). Nanometer-sized pores can now be etched on this

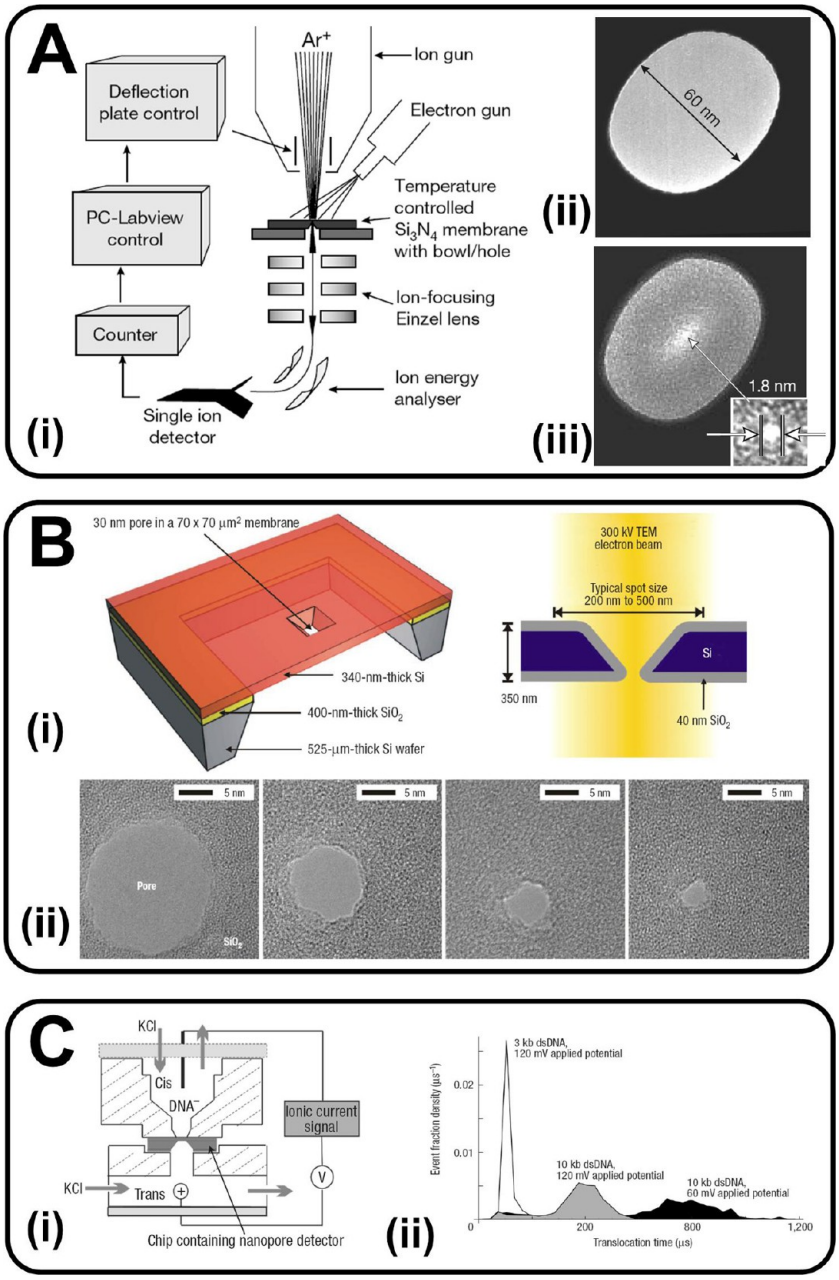

Figure 9. (A) (i) Feedback-controlled ion beam sculpting setup. A differentially pumped Ar^+ ion beam etches nanopores in thin Si_3N_4 membranes. (ii) Transmission electron micrograph (TEM) image of a 60 nm nanopore etched in a 500 nm silicon nitride membrane. (iii) TEM image of the same pore after Ar^+ ion beam exposure to shrink the pore size down to 1.8 nm. Reprinted with permission from ref 192. Copyright 2001 Macmillan Publishers Ltd. (B) (i) Cross-section view of solid-state nanopore fabricated in silicon oxide. Pyramid-shaped pores patterned on free-standing single-crystalline silicon membranes supported on KOH-etched silicon wafers are reduced to nanopores by thermal oxidation of silicon. The pores are about 20 × 20 nm^2 surrounded by a 40 nm thick SiO_2 layer. (ii) Sequential TEM images showing the shrinking of the 20 nm nanopore to 3 nm in size by exposure to focused electron irradiation. Reproduced with permission from ref 193. Copyright 2003 Macmillan Publishers Ltd. (C) (i) Translocation of DNA molecules across a solid-state nanopore. The nanopore membrane is placed between two electrolytes with a voltage applied across the membrane. Individual DNA and protein molecules are driven through the nanopore and, by monitoring change in ionic current, allow one to measure the translocation time through the pore. (ii) Translocation time distribution as a function of DNA size across a 10 nm solid-state nanopore. The plot shows the translocation time for a 3 and 10 kb dsDNA molecules at 120 mV bias, and for 10 kb dsDNA at 60 mV bias. Reproduced with permission from ref 198. Copyright 2003 Macmillan Publishers Ltd.

free-standing membrane by using high intensity focused beams of ions or electrons.[192,193] The size of the pore can be controlled by varying the intensity of the focused ion or electron beam as well as other factors including exposure time and temperature. Golovchenko's groups at Harvard reported perhaps the first demonstration of fabricating these nanopore membranes using focused ion beams.[192] Using argon ion sputtering, they initially etched a 60 nm pore in a silicon nitride membrane. They then employed diffusion ion beam and

temperature-dependent material properties to tune the size of this nanopore down to 1.8 nm (see Figure 9A).[192] Recently, researchers have relied on high intensity focused electron beams to drill nanopores into Si_3N_4/SiO_2 membranes. This technique was first developed by Dekker and colleagues, where they employed the electron beam in a transmission electron microscope (TEM) to drill as well as reduce the size of larger pores in SiO_2 membranes (Figure 9B).[193] The group first fabricated larger pores (up to 200 nm in size) using electron beam lithography followed by reactive ion etching and wet KOH etching. Exposing these larger pores to an electron beam of 10^5 to 10^7 A m^{-2} intensity causes the pores to either shrink or expand depending on the initial pore diameter. For example, the authors reported that pores with an initial diameter of 50 nm or lesser shrink upon exposure to the electron beam, while pores with >80 nm initial diameter expand under the same conditions. This technique can hence be used to fine-tune pore sizes to achieve single nanometer precision. The shrinking of pores when exposed to a high intensity electron beam is explained by the fluidization of the SiO_2 layer causing the pore to collapse under surface tension.[193] Deposition of highly conformal films/coatings can also be used to fine-tune and control the size of nanopores. For example, Chen and co-workers[194] used atomic layer deposition of conformal aluminum oxide films to shrink the size of larger nanopores prefabricated using ion beam sculpting. Such techniques offer better control over pore dimensions by controlling the deposition cycle as well as allow surface modification for various sensing applications.[189,195]

The ability to control single-molecule transport through these solid-state nanopores offers limitless possibilities for the study and detection of biomolecules including DNA, RNA, and proteins. These membranes have been primarily used for the translocation of individual DNA molecules through the nanopores.[183,184,196−199] By placing the nanopore membrane between two electrolytes and applying a voltage across them, individual molecules can be driven through the nanoscale pore. Monitoring the change in ionic current allows one to measure the time to translocate through the pore. This method can hence be applied to size DNA molecules based on their lengths, analogous to gel electrophoresis (see Figure 9C).[198] A significant advantage of using a nanopore as opposed to gel electrophoresis is the ability to work with much smaller sample volumes (~1000 molecules). Reducing the pore size to the order of a couple of nanometers allows only single-stranded DNA (ssDNA) to pass through the pores. Such a method has the potential to compete with future generations of DNA sequencing technologies, with the promise of sequencing the human genome for under $1000.[187,188] However, this is challenging as it is required that the initial DNA sequence be modified for detection and read-out. Second, as the ssDNA moves through the nanopore at very high velocities, much work in the areas of detection techniques based on either electrical sensing (tunneling current, capacitance) or optical read-out is warranted. As a first step, techniques to slow DNA translocation through nanopores have been reported.[200] Finally, these nanopore membranes can also be used as an imaging tool to provide ultrahigh magnification to observe DNA molecules and their configurations.[198]

Apart from using solid-state technology, single-nanopore membranes have been fabricated in glass and quartz materials.[201−203] To fabricate nanopores in glass, first, chemically sharpened platinum or gold metal wires are embedded in a macroglass capillary, followed by glass softening around the metal wire. Next, mechanical polishing is performed to remove the excess glass materials and expose the nanometer-sized tip of the metal wire. Finally, chemical etching to remove the metal wire leaves a conical nanopore at the end of the glass capillary.[201] Applications including nanoparticle transport and single-ion channel recording using these nanopore membranes have been shown.[202,203]

Although solid-state fabrication technology for making nanopores has made rapid progress in the past decade, the technology does not lend itself well for making arrays of nanopores and is typically limited to single-pore events. To overcome this limitation, ion track-etching commonly used for making microporous membranes has been employed to fabricate nanoporous membranes in silicon nitride.[204] Using high-energy bismuth ions to create damaged tracks followed by chemical etching, conical and double-conical nanoporous membranes with pore diameters as small as 4 nm were fabricated. Similar technique can also be used to fabricate nanoporous membranes in polymer materials such as PET and Kapton films.[205,206] Since the polymer films are much thicker (8−12 μm) than silicon nitride membranes used in solid-state fabrication methods (~300 nm), the nanopores have a very high aspect ratio and a distinct conical shape. The high aspect ratio of these pores provides higher temporal resolution of DNA fragments during translocation, thus allowing the detection of smaller fragments than that possible by solid-state nanopores.[21,206]

Isoporous Membranes Fabricated by Block Copolymer Self-Assembly. Block copolymers, macromolecules with long, covalently connected blocks of two or more distinct repeating units of the same monomer, have received great attention over the past decade for their unique ability to self-assemble and form complex structures with micro- and nanoscale feature sizes.[207−209] Depending on the volume fraction of the components, they can perfectly self-assemble into highly ordered arrays of nanoscopic domains with varying morphologies such as spheres, lamellae, and cylinders.[210] Various approaches, including use of electrical field,[211,212] crystallization,[213] magnetic biases,[214] and temperature gradient,[215] have been employed for precise control of orientation and architecture of the nanoscale domains.

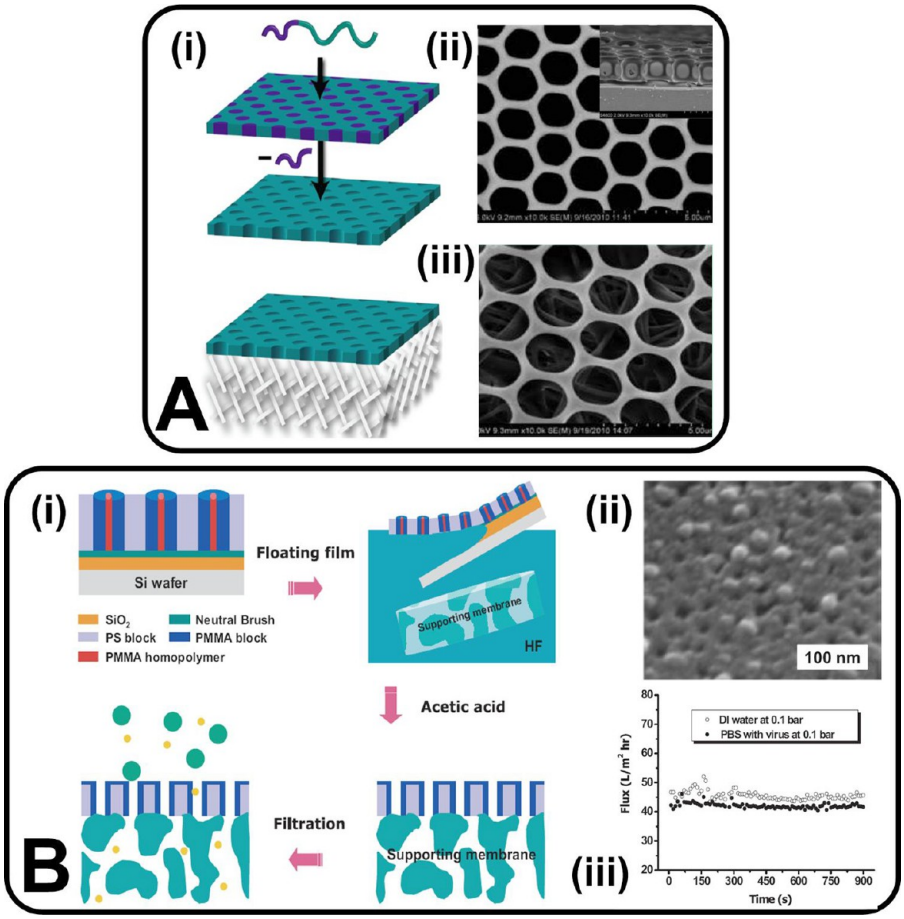

Figure 10. (A) (i) Schematic representation of the formation of isoporous nanoporous membranes from ordered block copolymers by selective etching of the minority domains (purple) from majority component (green). (ii,iii) SEM images of the typical ordered membrane with through-pores placed on a macroporous support. Reprinted from refs 207 and 209. Copyright 2004 American Chemical Society. B (i) Schematic illustration of the process for the fabrication of an isoporous nanoporous membrane using block copolymers. The process starts with casting of the mixture of PS-*b*-PMMA on a Si substrate followed by dissolution of a sacrificial layer in HF. The floated film on the HF solution is transferred to a microporous supporting membrane, and the final nanoporous membrane is achieved by dissolving the PMMA homopolymer selectively in an acetic acid solution. (ii) SEM image of a nanoporous membrane after filtration of a solution containing human rhinovirus type 14 (HRV14). (iii) Ultrafiltration data using DI water and PBS solution containing HRV14 using the aforementioned nanoporous membrane. Reprinted with permission from ref 219. Copyright 2006 Wiley-VCH Verlag GmbH & Co. KGaA.

An overview of block copolymers to generate isoporous membranes that can be used in applications such as ultrafiltration, drug delivery, and nanolithography will be briefly discussed in this section.

Block copolymers are hybrid macromolecules that are classified based on the number of blocks they contain and how the blocks are arranged.[216] They are normally prepared by controlled polymerization of one monomer, followed by chain extension with a different monomer to form AB diblock or ABC triblock architectures. The pairs of monomers can be a combination of conducting materials,[217] ligands,[218] metal-containing segments, and degradable (etchable) components.[216] The latter set of materials, which is part of the most common strategy to fabricate nanoporous membranes, involves selective dissolution of the minority component typically embedded in the majority components in a thin film of a block copolymer (Figure 10A).[207] Figure 10B schematically shows typical fabrication of asymmetric isoporous membranes using block copolymers. The process begins with casting of a mixture of block copolymers such as PS-*b*-PMMA (polystyrene-*block*-poly(methyl methacrylate)), with cylindrical nanodomains of PMMA, on a Si substrate which was initially covered by a thin film of SiO_2 as a sacrificial layer.[219] By adding the PMMA homopolymer to the PS-*b*-PMMA block copolymer, it can preferentially segregate to the center of the cylindrical PMMA nanodomains and orient normal to the surface in the film. This thin film can be released from the substrate by dissolving the sacrificial layer (*i.e.*, SiO_2) in a buffered HF acid solution. To safeguard the membrane during handling and filtration, the thin film can be placed on a polysulfone (PSU) membrane with large openings. In the last step, an isoporous nanoporous membrane with pore sizes down to 15 nm can be achieved by dissolving the PMMA homopolymer selectively in an acetic acid (nonsolvent for the PS) solution.[219] The size of the pores can be controlled by

the molecular weight, architecture of the blocks, volume fraction, segmental interactions, as well as process parameters.

The combination of new synthetic methods with an understanding of phase behavior shows that, by simple manipulation of block copolymers, nanoporous materials with cylindrical nanochannels can be produced for various advanced technologies such as nanolithography,[220] water purification,[221] and drug delivery.[222] For example, Yang *et al.*[219] employed an asymmetric nanoporous membrane fabricated with block copolymers for separation of human rhinovirus type 14 (HRV14). They have successfully demonstrated the sized-based removal of HRV14 rhinovirus with a high flux from an aqueous dispersion which showed significantly higher performance (100-fold higher) than the polycarbonate track-etched membranes (see Figure 10B). The same nanoporous membrane with tailored pore size (*i.e.*, using gold sputtering) has been used recently for drug delivery applications by other researchers.[30] They have shown the application of isoporous membranes made with self-assembly of block copolymers for long-term controlled release of therapeutic proteins such as bovine serum albumin (BSA) and hGH using a single-file diffusion (SFD) mechanism. These examples demonstrate highly reliable and tunable separations made possible by employing block copolymer membranes. Combining the advantages of microfabrication and block copolymers, Nuxoll *et al.*[67] fabricated a robust composite membrane recently, providing both nanoscale size exclusion and fast transport of small molecules. They could also effectively trigger the transport of macromolecules through the membrane by tuning the membrane chemically using comonomers such as glycolide in the initial block copolymer components. In another study, Peinemann's group developed a novel process to produce pH-responsive nanoporous membranes for ultrafiltration (UF), by combining the metal block copolymer complexes and phase inversion technique.[223] For a more complete and detailed discussion about block copolymers and their applications, the reader is encouraged to refer to comprehensive reviews by Hillmyer and colleagues.[207,216,224]

Particle-assisted wetting (or float-casting) is another attractive self-assembly approach which has been developed by Xu *et al.*[225,226] for fabrication of ultrathin free-standing porous membranes. In this technique, a mixture of nanosized spherical particles coated with a hydrophobic polymer and a non-water-soluble, polymerizable liquid monomer is applied to a water surface. Eventually, this mixture forms a monolayer of colloids on the water surface that are embedded in a layer of the liquid monomer. After cross-linking of monomer using photopolymerization and removal of particles, a free-standing membrane containing pores with similar diameter to the colloids can be formed. Structures with very narrow pore size distribution and small pore diameters (50−100 nm) can be obtained with this technique. Recently, Yan *et al.*[227] combined phase separation micromolding and float-casting to prepare an isoporous nanosieve with hierarchically structured support for filtration applications. In another example, Jahn and colleagues[228] developed a new technique called "inkjet printing" where they employed water droplets as a template to create micrometer-sized pores inside a polymeric solution (liquid PMMA) cast between the sessile drops of water on a hydrophobic substrate (aluminum foil).

Nanoporous membranes leveraging on the self-assembling microscopic fabrication of carbon nanotubes (CNTs) have also been used for filtration applications. The excellent thermal and mechanical properties of these membranes make them suitable for high flux, high-throughput filtration applications. The unique properties of these membranes with well-controlled pore size (down to 0.7 nm) provide significant advantage over other membrane technologies for water filtration and desalination. Furthermore, CNT membranes have a unique ability to adsorb many toxic chemicals and destroy microbial contaminants.[229] Non-isoporous CNT membranes formed by nonwoven structures, popularly known as Bucky paper, have been widely used historically. However, isoporous CNT membranes formed by encapsulating an upright standing CNT forest using an epoxy material are possible. Briefly, a forest of aligned CNTs is grown by traditional chemical vapor deposition (CVD) on silicon or quartz substrate. Following CNT deposition, the entire CNT forests are encapsulated with an impermeable material to form a continuous matrix/membrane. Next, the excess matrix material is removed by either polishing or plasma treatment. Last, the matrix with the CNTs is released from the substrate to form an isoporous membrane. These membranes have a very well-defined inner pore diameter and high pore density (typically $>10^{11}$ cm^{-2}) compared to typical track-etched membranes, leading to better permeance.[229,230]

Isoporous membranes produced with most self-assembly techniques are extremely uniform and have a smooth surface. Structures with very narrow pore size distribution and small pore diameters down to a few nanometers can be obtained with these approaches. Although a major hurdle in their use is the large-scale production because achieving a large defect-free surface area is difficult in these approaches. Furthermore, the pore sizes and shapes and their distribution cannot be controlled perfectly similar to MEMS techniques.

SUMMARY AND FUTURE PERSPECTIVE

Isoporous membranes with micro- and nanopore dimensions are currently being developed for various applications such as immunoisolation, dialysis, biosensors, and photonics. Advances in micro/nanofabrication and material synthesis techniques have significantly

enhanced the ability to control the microstructure of membrane materials, allowing fabrication of membranes with extremely high selectivity and superior mechanical and chemical stability. In this review, various techniques for fabrication of isoporous membranes have been summarized. Detailed fabrication procedures for these methodologies are outlined, including material considerations and pore geometries. The versatility of these structures has garnered interest from a range of scientific and industrial communities for its numerous potential applications in fields ranging from biological and medical science with applications in sorting, sensing, isolating, and releasing biological molecules to environmental applications including water filtration and contamination detection.

MEMS approaches (including solid-state nanopore), which normally use the mature microfabrication techniques, borrowed from the semiconductor industry can be utilized for large-scale (and defect-free) manufacturing of isoporous membranes using a wide range of organic and inorganic materials. The surface and pore size of these membranes can be modified and/or functionalized using polymer coating such as parylene or atomic layer deposition (ALD) and electroless plating techniques. A great advantage is also the possibility to integrate the isoporous membranes inside microfluidic (lab-on-chip) devices for point-of-care applications. However, the high capital and operating cost required for conventional microfabrication techniques (*e.g.*, mask fabrication, lithography, and sputtering) make these membranes rather expensive to fabricate. To overcome this, unconventional techniques such as micro/nanomolding, hot-embossing, and printing techniques have been developed and successfully employed for fabrication of high-yield and low-cost isoporous membranes. Electrochemical etching approach using anodization is also investigated extensively for fabrication of isoporous nanoporous membranes for various applications. Similar to MEMS techniques, nanoporous membranes derived from anodization have the potential to be extremely effective as separation (and/or controlled release) membranes given their very narrow pore size distributions and high porosities. Realization of a large and defect-free membrane coupled with the large thickness of these membranes due to their intrinsic fragility (*i.e.*, because of their oxide nature) usually limits their applications for high-throughput separations. Nanoporous membranes that are obtained from self-assembly of block copolymers are also pursued as attractive materials for sorting, sensing, and drug release applications due to their pore size tunability and ability for selective functionalization. The quality, efficacy, and applicability of these membranes have advanced considerably over the past decades; however, active research is still needed to develop processes that are more appealing for large-scale production.

Fabrication of versatile isoporous membranes is an integral step to realize their applications in numerous fields. Ease of manufacturing (*i.e.*, low-cost and high-yield), multiple functionalities (*e.g.*, size screening, pH-sensitive, biocompatible, and biofouling resistance), and reusability are key performance metrics for comparing the next generation of isoporous membranes. We strongly believe that exciting future advances in this field are yet to come, aided by advances in novel fabrication methods. Although modulating processing parameters and protocols will enable novel applications in this area, innovative nanofabrication approaches and development of new materials and composites will be centrally important in facilitating future progress in the field. For now, membrane science is well placed to play a pivotal role in various biological and medical applications. Other unique applications, such as 3D tissue engineering, biosensing, and biomimetic studies are being explored, stretching the field to new horizons.

Conflict of Interest: The authors declare no competing financial interest.

REFERENCES AND NOTES

1. Baker, R. W. *Membrane Technology and Applications*, 2nd ed.; John Wiley & Sons: West Sussex, England, 2004.
2. Van Rijn, C. *Nano and Micro Engineered Membrane Technology*: Elsevier Science: Amsterdam, The Netherlands, 2004.
3. Striemer, C. C.; Gaborski, T. R.; McGrath, J. L.; Fauchet, P. M. Charge- and Size-Based Separation of Macromolecules Using Ultrathin Silicon Membranes. *Nature* **2007**, *445*, 749–753.
4. Wright, D.; Rajalingam, B.; Karp, J. M.; Selvarasah, S.; Ling, Y.; Yeh, J.; Langer, R.; Dokmeci, M. R.; Khademhosseini, A. Reusable, Reversibly Sealable Parylene Membranes for Cell and Protein Patterning. *J. Biomed. Mater. Res., Part A* **2008**, *85*, 530–538.
5. Zheng, Y.; Dai, W.; Ryan, D.; Wu, H. Fabrication of Free-standing, Microperforated Membranes and Their Applications in Microfluidics. *Biomicrofluidics* **2010**, *4*, 036504.
6. Masuda, H.; Yasui, K.; Nishio, K. Fabrication of Ordered Arrays of Multiple Nanodots Using Anodic Porous Alumina as an Evaporation Mask. *Adv. Mater.* **2000**, *12*, 1031–1033.
7. Adiga, S. P.; Curtiss, L. A.; Elam, J. W.; Pellin, M. J.; Shih, C. C.; Shih, C. M.; Lin, S. J.; Su, Y. Y.; Gittard, S. D.; Zhang, J. Nanoporous Materials for Biomedical Devices. *JOM* **2008**, *60*, 26–32.
8. Adiga, S. P.; Jin, C.; Curtiss, L. A.; Monteiro-Riviere, N. A.; Narayan, R. J. Nanoporous Membranes for Medical and Biological Applications. *Wiley Interdiscip. Rev.: Nanomed. Nanobiotechnol.* **2009**, *1*, 568–581.
9. Zhu, B.; Li, J.; Xu, D. Porous Biomimetic Membranes: Fabrication, Properties and Future Applications. *Phys. Chem. Chem. Phys.* **2011**, *13*, 10584–10592.
10. Leoni, L.; Attiah, D.; Desai, T. A. Nanoporous Platforms for Cellular Sensing and Delivery. *Sensors* **2002**, *2*, 111–120.
11. Martin, C. R.; Siwy, Z. S. Learning Nature's Way: Biosensing with Synthetic Nanopores. *Science* **2007**, *317*, 331–332.
12. Warkiani, M. E.; Chen, L.; Lou, C. P.; Liu, H. B.; Zhang, R.; Gong, H. Q. Capturing and Recovering of *Cryptosporidium parvum* Oocysts with Polymeric Micro-fabricated Filter. *J. Membr. Sci.* **2011**, *369*, 560–568.
13. Zavala-Rivera, P.; Channon, K.; Nguyen, V.; Sivaniah, E.; Kabra, D.; Friend, R. H.; Nataraj, S.; Al-Muhtaseb, S. A.;

Hexemer, A.; Calvo, M. E. Collective Osmotic Shock in Ordered Materials. *Nat. Mater.* **2011**, *11*, 53–57.
14. Ramachandran, V.; Fogler, H. S. Plugging by Hydrodynamic Bridging during Flow of Stable Colloidal Particles within Cylindrical Pores. *J. Fluid Mech.* **1999**, *385*, 129–156.
15. Buyukserin, F.; Kang, M.; Martin, C. R. Plasma-Etched Nanopore Polymer Films and Their Use as Templates To Prepare "Nano Test Tubes". *Small* **2007**, *3*, 106–110.
16. Mitchell, D. T.; Lee, S. B.; Trofin, L.; Li, N.; Nevanen, T. K.; Söderlund, H.; Martin, C. R. Smart Nanotubes for Bioseparations and Biocatalysis. *J. Am. Chem. Soc.* **2002**, *124*, 11864–11865.
17. Guo, P.; Martin, C. R.; Zhao, Y.; Ge, J.; Zare, R. N. General Method for Producing Organic Nanoparticles Using Nanoporous Membranes. *Nano Lett.* **2010**, *10*, 2202–2206.
18. Wirtz, M.; Martin, C. R. Template-Fabricated Gold Nanowires and Nanotubes. *Adv. Mater.* **2003**, *15*, 455–458.
19. Li, N.; Yu, S.; Harrell, C. C.; Martin, C. R. Conical Nanopore Membranes. Preparation and Transport Properties. *Anal. Chem.* **2004**, *76*, 2025–2030.
20. Li, J.; Wang, Q.; Gu, C. Growth and Field Emission Properties of Tubular Carbon Cones. *Ultramicroscopy* **2007**, *107*, 861–864.
21. Sexton, L. T.; Horne, L. P.; Martin, C. R. Developing Synthetic Conical Nanopores for Biosensing Applications. *Mol. BioSyst.* **2007**, *3*, 667–685.
22. Mukaibo, H.; Horne, L. P.; Park, D.; Martin, C. R. Controlling the Length of Conical Pores Etched in Ion-Tracked Poly(ethylene terephthalate) Membranes. *Small* **2009**, *5*, 2474–2479.
23. Zang, J.; Bao, S.-J.; Li, C. M.; Bian, H.; Cui, X.; Bao, Q.; Sun, C. Q.; Guo, J.; Lian, K. Well-Aligned Cone-Shaped Nanostructure of Polypyrrole/Ruo2 and Its Electrochemical Supercapacitor. *J. Phys. Chem. C* **2008**, *112*, 14843–14847.
24. Gates, B. D.; Xu, Q.; Stewart, M.; Ryan, D.; Willson, C. G.; Whitesides, G. M. New Approaches to Nanofabrication: Molding, Printing, and Other Techniques. *Chem. Rev.* **2005**, *105*, 1171–1196.
25. Stroeve, P.; Ileri, N. Biotechnical and Other Applications of Nanoporous Membranes. *Trends Biotechnol.* **2011**, *29*, 259–266.
26. Fryd, M. M.; Mason, T. G. Advanced Nanoemulsions. *Annu. Rev. Phys. Chem.* **2012**, *63*, 493–518.
27. Geerken, M. J.; van Zanten, T. S.; Lammertink, R. G. H.; Borneman, Z.; Nijdam, W.; Van Rijn, C. J. M.; Wessling, M. Chemical and Thermal Stability of Alkylsilane Based Coatings for Membrane Emulsification. *Adv. Eng. Mater.* **2004**, *6*, 749–754.
28. Fu, J.; Mao, P.; Han, J. Artificial Molecular Sieves and Filters: A New Paradigm for Biomolecule Separation. *Trends Biotechnol.* **2008**, *26*, 311–320.
29. Chilkoti, A.; Dreher, M. R.; Meyer, D. E.; Raucher, D. Targeted Drug Delivery by Thermally Responsive Polymers. *Adv. Drug Delivery Rev.* **2002**, *54*, 613–630.
30. Yang, S. Y.; Yang, J. A.; Kim, E. S.; Jeon, G.; Oh, E. J.; Choi, K. Y.; Hahn, S. K.; Kim, J. K. Single-File Diffusion of Protein Drugs through Cylindrical Nanochannels. *ACS Nano* **2010**, *4*, 3817–3822.
31. Warkiani, M. E.; Lou, C. P.; Liu, H. B.; Gong, H. Q. A High-Flux Isopore Micro-fabricated Membrane for Effective Concentration and Recovering of Waterborne Pathogens. *Biomed. Microdevices* **2012**, 1–9.
32. Holm, S. H.; Beech, J. P.; Barrett, M. P.; Tegenfeldt, J. O. Separation of Parasites from Human Blood Using Deterministic Lateral Displacement. *Lab Chip* **2011**, *11*, 1326–1332.
33. De Jong, J.; Lammertink, R.; Wessling, M. Membranes and Microfluidics: A Review. *Lab Chip* **2006**, *6*, 1125–1139.
34. Tan, S. J.; Yobas, L.; Lee, G. Y. H.; Ong, C. N.; Lim, C. T. Microdevice for the Isolation and Enumeration of Cancer Cells from Blood. *Biomed. Microdevices* **2009**, *11*, 883–892.
35. Franssila, S. *Introduction to Microfabrication*; Wiley Online Library, 2004.
36. Vogelaar, L. Phase Separation Micromolding. PhD Dissertation, University of Twente, Enschede, The Netherlands, 2005.
37. http://www.etchform.com/.
38. Schuster-Woldan, K.; Weingard, K.; Koch, D. Process for Producing a Thin Metal Structure with a Self-Supporting Frame. U.S. Patent 4058432, 1977.
39. http://www.spgveco.com/.
40. Ehrfeld, W.; Einhaus, R.; Münchmeyer, D.; Strathmann, H. Microfabrication of Membranes with Extreme Porosity and Uniform Pore Size. *J. Membr. Sci.* **1988**, *36*, 67–77.
41. Taguchi, T.; Arakaki, A.; Takeyama, H.; Haraguchi, S.; Yoshino, M.; Kaneko, M.; Ishimori, Y.; Matsunaga, T. Detection of *Cryptosporidium parvum* Oocysts Using a Microfluidic Device Equipped with the Sus Micromesh and FITC-Labeled Antibody. *Biotechnol. Bioeng.* **2007**, *96*, 272–280.
42. Hosokawa, M.; Hayata, T.; Fukuda, Y.; Arakaki, A.; Yoshino, T.; Tanaka, T.; Matsunaga, T. Size-Selective Microcavity Array for Rapid and Efficient Detection of Circulating Tumor Cells. *Anal. Chem.* **2010**, *82*, 6629–6635.
43. Madou, M. J. *Fundamentals of Microfabrication: The Science of Miniaturization*; CRC Press: Boca Raton, FL, 2002.
44. Stemme, G.; Kittilsland, G. New Fluid Filter Structure in Silicon Fabricated Using a Self-Aligning Technique. *Appl. Phys. Lett.* **1988**, *53*, 1566–1568.
45. Kittilsland, G.; Stemme, G.; Norden, B. A Sub-Micron Particle Filter in Silicon. *Sens. Actuators, A* **1990**, *23*, 904–907.
46. Chu, W. H.; Ferrari, M. In *Silicon Nanofilter with Absolute Pore Size and High Mechanical Strength*, Proc. SPIE 2593, Microrobotics and Micromechanical Systems, December 18, **1995**, p 9.
47. Chu, W. H.; Chin, R.; Huen, T.; Ferrari, M. Silicon Membrane Nanofilters from Sacrificial Oxide Removal. *J. Microelectromech. Syst.* **1999**, *8*, 34–42.
48. Chu, W.; Huen, T.; Tu, J.; Ferrari, M. Silicon-Micromachined Direct-Pore Filters for Ultrafiltration. *J. Soc. Photo-Opt. Instrum. Eng.* **1997**, *2978*, 111–122.
49. Martin, F.; Walczak, R.; Boiarski, A.; Cohen, M.; West, T.; Cosentino, C.; Ferrari, M. Tailoring Width of Microfabricated Nanochannels to Solute Size Can Be Used To Control Diffusion Kinetics. *J. Controlled Release* **2005**, *102*, 123–133.
50. Desai, T. A.; Hansford, D.; Ferrari, M. Characterization of Micromachined Silicon Membranes for Immunoisolation and Bioseparation Applications. *J. Membr. Sci.* **1999**, *159*, 221–231.
51. Desai, T. A.; Hansford, D. J.; Ferrari, M. Micromachined Interfaces: New Approaches in Cell Immunoisolation and Biomolecular Separation. *Biomol. Eng.* **2000**, *17*, 23–36.
52. Walczak, R. J.; Boiarski, A.; Cohen, M.; West, T.; Melnik, K.; Shapiro, J.; Sharma, S.; Ferrari, M. Long-Term Biocompatibility of Nanogate Drug Delivery Implant. *NanoBiotechnology* **2005**, *1*, 35–42.
53. Fissell, W. H.; Dubnisheva, A.; Eldridge, A. N.; Fleischman, A. J.; Zydney, A. L.; Roy, S. High-Performance Silicon Nanopore Hemofiltration Membranes. *J. Membr. Sci.* **2009**, *326*, 58–63.
54. Ogura, E.; Kusumoputro, B.; Moriizumi, T. Passage Time Measurement of Individual and Blood Cells through Arrayed Micropores on Si3N4 Membrane. *J. Biomed. Eng.* **1991**, *13*, 503–506.
55. Ogura, E.; Abatti, P. J.; Moriizumi, T. Measurement of Human Red Blood Cell Deformability Using a Single Micropore on a Thin Si_3N_4 Film. *IEEE Trans. Biomed. Eng.* **1991**, *38*, 721–726.
56. Rijn, C. J. M.; Nijdam, W.; Elwenspoek, M. High Flowrate Microsieve for Biomedical Applications. *ASME Dyn. Syst. Control Conf., Proc.* **1995**.
57. Kuiper, S.; Van Rijn, C. J. M.; Nijdam, W.; Elwenspoek, M. C. Development and Applications of Very High Flux Microfiltration Membranes. *J. Membr. Sci.* **1998**, *150*, 1–8.

58. Kuiper, S.; Brink, R.; Nijdam, W.; Krijnen, G.; Elwenspoek, M. Ceramic Microsieves: Influence of Perforation Shape and Distribution on Flow Resistance and Membrane Strength. *J. Membr. Sci.* **2002**, *196*, 149–157.
59. Kuiper, S.; Boer, M.; Rijn, C.; Nijdam, W.; Krijnen, G.; Elwenspoek, M. Wet and Dry Etching Techniques for the Release of Sub-micrometre Perforated Membranes. *J. Micromech. Microeng.* **2000**, *10*, 171.
60. Rijn, C. J. M.; Veldhuis, G. J.; Kuiper, S. Nanosieves with Microsystem Technology for Microfiltration Applications. *Nanotechnology* **1998**, *9*, 343.
61. Sainiemi, L.; Viheriälä, J.; Sikanen, T.; Laukkanen, J.; Niemi, T. Nanoperforated Silicon Membranes Fabricated by UV-Nanoimprint Lithography, Deep Reactive Ion Etching and Atomic Layer Deposition. *J. Micromech. Microeng.* **2010**, *20*, 077001.
62. Nabar, B. P.; Çelik-Butler, Z.; Dennis, B. H.; Billo, R. E. A Nanoporous Silicon Nitride Membrane Using a Two-Step Lift-Off Pattern Transfer with Thermal Nanoimprint Lithography. *J. Micromech. Microeng.* **2012**, *22*, 045012.
63. Kuiper, S.; Van Rijn, C.; Nijdam, W.; Raspe, O.; van Wolferen, H.; Krijnen, G.; Elwenspoek, M. Filtration of Lager Beer with Microsieves: Flux, Permeate Haze and In-Line Microscope Observations. *J. Membr. Sci.* **2002**, *196*, 159–170.
64. Wu, J.; Zhang, M.; Chen, L.; Yu, V.; Wong, J. T. Y.; Zhang, X.; Qin, J.; Wen, W. Patterning Cell Using Si-Stencil for High-Throughput Assay. *RSC Adv.* **2011**, *1*, 746–750.
65. Rijn, C. J. M.; Nijdam, W.; Kuiper, S.; Veldhuis, G. J.; Wolferen, H.; Elwenspoek, M. Microsieves Made with Laser Interference Lithography for Micro-filtration Applications. *J. Micromech. Microeng.* **1999**, *9*, 170.
66. Popa, A. M.; Niedermann, P.; Heinzelmann, H.; Hubbell, J. A.; Pugin, R. Fabrication of Nanopore Arrays and Ultrathin Silicon Nitride Membranes by Block-Copolymer-Assisted Lithography. *Nanotechnology* **2009**, *20*, 485303.
67. Nuxoll, E. E.; Hillmyer, M. A.; Wang, R.; Leighton, C.; Siegel, R. A. Composite Block Polymer–Microfabricated Silicon Nanoporous Membrane. *ACS Appl. Mater. Interfaces* **2009**, *1*, 888–893.
68. Klein, M. J. K.; Montagne, F.; Blondiaux, N.; Vazquez-Mena, O.; Heinzelmann, H.; Pugin, R.; Brugger, J.; Savu, V. SiN Membranes with Submicrometer Hole Arrays Patterned by Wafer-Scale Nanosphere Lithography. *J. Vac. Sci. Technol., B* **2011**, *29*, 021012–021015.
69. Lee, D. S.; Song, H. W.; Chung, K. H.; Jung, M. Y.; Yoon, H. C. Microfabrication of SiN Membrane Nanosieve Using Anisotropic Reactive Ion Etching (Arie) with an Ar/Cf4 Gas Flow. *J. Nanosci. Nanotechnol.* **2011**, *11*, 4511–4516.
70. Heyderman, L.; Ketterer, B.; Bächle, D.; Glaus, F.; Haas, B.; Schift, H.; Vogelsang, K.; Gobrecht, J.; Tiefenauer, L.; Dubochet, O. High Volume Fabrication of Customised Nanopore Membrane Chips. *Microelectron. Eng.* **2003**, *67*, 208–213.
71. Van den Boogaart, M.; Kim, G.; Pellens, R.; Van den Heuvel, J. P.; Brugger, J. Deep-Ultraviolet–Microelectromechanical Systems Stencils for High-Throughput Resistless Patterning of Mesoscopic Structures. *J. Vac. Sci. Technol., B* **2004**, *22*, 3174–3178.
72. Zhang, W.; Li, J.; Cao, L.; Wang, Y.; Guo, W.; Liu, K.; Xue, J. Fabrication of Nanoporous Silicon Dioxide/Silicon Nitride Membranes Using Etched Ion Track Technique. *Nucl. Instrum. Methods Phys. Res., Sect. B* **2008**, *266*, 3166–3169.
73. Tong, H. D.; Gielens, F.; Gardeniers, J.; Jansen, H. V.; Berenschot, J.; de Boer, M. J.; De Boer, J.; Van Rijn, C. J. M.; Elwenspoek, M. C. Microsieve Supporting Palladium–Silver Alloy Membrane and Application to Hydrogen Separation. *J. Microelectromech. Syst.* **2005**, *14*, 113–124.
74. Gielens, F.; Tong, H.; Van Rijn, C.; Vorstman, M.; Keurentjes, J. Microsystem Technology for High-Flux Hydrogen Separation Membranes. *J. Membr. Sci.* **2004**, *243*, 203–213.
75. Wagdare, N. A.; Marcelis, A.; Ho, O. B.; Boom, R. M.; Van Rijn, C. J. M. High Throughput Vegetable Oil-in-Water Emulsification with a High Porosity Micro-engineered Membrane. *J. Membr. Sci.* **2010**, *347*, 1–7.
76. Yang, X.; Yang, J. M.; Tai, Y. C.; Ho, C. M. Micromachined Membrane Particle Filters. *Sens. Actuators, A* **1999**, *73*, 184–191.
77. Hsiai, T. K.; Cho, S. K.; Yang, J. M.; Yang, X.; Tai, Y. C.; Ho, C. M. Pressure Drops of Water Flow through Micromachined Particle Filters. *J. Fluids Eng.* **2002**, *124*, 1053.
78. Geerken, M.; Lammertink, R.; Wessling, M. Tailoring Surface Properties for Controlling Droplet Formation at Microsieve Membranes. *Colloids Surf., A* **2007**, *292*, 224–235.
79. Heller, C.; Reidt, U.; Helwig, A.; Müller, G.; Meixner, L.; Neumeier, K.; Lindner, P.; Molz, R.; Wolf, H.; Zullei-Seibert, N. In *Fast Detection and Identification of Bacteria in Potable Water*, Proceedings of SPIE, May 8, **2009**, p 730406.
80. Vaeth, K. M. Micromachined Microsieves with High Aspect Ratio Features. *J. Microelectromech. Syst.* **2012**, 1–8.
81. Venstra, W.; Pham, N.; Sarro, P.; Van Eijk, J. Particle Filters Integrated inside a Silicon Wafer. *Microelectron. Eng.* **2005**, *78*, 138–141.
82. Modroukas, D.; Modi, V.; Fréchette, L. G. Micromachined Silicon Structures for Free-Convection PEM Fuel Cells. *J. Micromech. Microeng.* **2005**, *15*, S193.
83. Kuiper, S. Development and Application of Microsieves. PhD Dissertation, University of Twente, Enschede, The Netherlands, 2000.
84. Girones, M.; Akbarsyah, I.; Nijdam, W.; Van Rijn, C.; Jansen, H.; Lammertink, R.; Wessling, M. Polymeric Microsieves Produced by Phase Separation Micromolding. *J. Membr. Sci.* **2006**, *283*, 411–424.
85. Brauker, J. H.; Martinson, L. A.; Sternberg, S.; Bellamy, D. Porous Microfabricated Polymer Membrane Structures. U.S. Patent 5807406, 1998.
86. Ramakrishna, S.; Ma, Z.; Matsuura, T. *Polymer Membranes in Biotechnology: Preparation, Functionalization and Application*; Imperial College Press: London, 2009.
87. Warkiani, M. E.; Lou, C. P.; Gong, H. Q. Fabrication and Characterization of a Microporous Polymeric Micro-filter for Isolation of *Cryptosporidium parvum* Oocysts. *J. Micromech. Microeng.* **2011**, *21*, 035002.
88. Warkiani, M. E.; Lou, C. P.; Gong, H. Q. Fabrication of Multi-layer Polymeric Micro-sieve Having Narrow Slot Pores with Conventional Ultraviolet-Lithography and Micro-Fabrication Techniques. *Biomicrofluidics* **2011**, *5*, 036504.
89. Gutierrez-Rivera, L. E.; Cescato, L. SU-8 Submicrometric Sieves Recorded by UV Interference Lithography. *J. Micromech. Microeng.* **2008**, *18*, 115003.
90. Elman, N. M.; Daniel, K.; Jalali-Yazdi, F.; Cima, M. J. Super Permeable Nano-channel Membranes Defined with Laser Interferometric Lithography. *Microfluid. Nanofluid.* **2010**, *8*, 557–563.
91. Prenen, A. M.; Van Der Werf, J.; Bastiaansen, C. W. M.; Broer, D. J. Monodisperse, Polymeric Nano- and Microsieves Produced with Interference Holography. *Adv. Mater.* **2009**, *21*, 1751–1755.
92. Makarova, O. V.; Tang, C. M.; Amstutz, P.; Divan, R.; Imre, A.; Mancini, D. C.; Hoffbauer, M.; Williamson, T. Fabrication of High Density, High-Aspect-Ratio Polyimide Nanofilters. *J. Vac. Sci. Technol., B* **2009**, *27*, 2585–2587.
93. Choi, J.; Roychowdhury, A.; Kim, N.; Nikitopoulos, D. E.; Lee, W.; Han, H.; Park, S. A Microfluidic Platform with a Free-Standing Perforated Polymer Membrane. *J. Micromech. Microeng.* **2010**, *20*, 085011.
94. Han, K.; Xu, W.; Ruiz, A.; Ruchhoeft, P.; Chellam, S. Fabrication and Characterization of Polymeric Microfiltration Membranes Using Aperture Array Lithography. *J. Membr. Sci.* **2005**, *249*, 193–206.
95. Zheng, S.; Lin, H. K.; Lu, B.; Williams, A.; Datar, R.; Cote, R. J.; Tai, Y. C. 3D Microfilter Device for Viable Circulating Tumor Cell (CTC) Enrichment from Blood. *Biomed. Microdevices* **2011**, *13*, 203–213.
96. Lu, B.; Xu, T.; Zheng, S.; Goldkorn, A.; Tai, Y. C. Parylene Membrane Slot Filter for the Capture, Analysis and

Culture of Viable Circulating Tumor Cells. *Proc. - IEEE Micro Electro Mech. Syst.* **2010**, 935–938.
97. Zheng, S.; Lin, H.; Liu, J. Q.; Balic, M.; Datar, R.; Cote, R. J.; Tai, Y. C. Membrane Microfilter Device for Selective Capture, Electrolysis and Genomic Analysis of Human Circulating Tumor Cells. *J. Chromatogr., A* **2007**, *1162*, 154–161.
98. Chen, W.; Lam, R. H. W.; Fu, J. Photolithographic Surface Micromachining of Polydimethylsiloxane (PDMS). *Lab Chip* **2011**, *12*, 391–395.
99. Huang, N. T.; Chen, W.; Oh, B. R.; Cornell, T. T.; Shanley, T. P.; Fu, J.; Kurabayashi, K. An Integrated Microfluidic Platform for *In-Situ* Cellular Cytokine Secretion Immunophenotyping. *Lab Chip* **2012**, *12*, 4093–4101.
100. Marzolin, C.; Smith, S. P.; Prentiss, M.; Whitesides, G. M. Fabrication of Glass Microstructures by Micro-molding of Sol−Gel Precursors. *Adv. Mater.* **1998**, *10*, 571–574.
101. Bikel, M.; Culfaz, P. Z.; Bolhuis-Versteeg, L.; Perez, J. G.; Lammertink, R.; Wessling, M. Polymeric Microsieves *via* Phase Separation Microfabrication: Process and Design Optimization. *J. Membr. Sci.* **2010**, *347*, 93–100.
102. Chen, L.; Warkiani, M. E.; Liu, H. B.; Gong, H. Q. Polymeric Micro-Filter Manufactured by a Dissolving Mold Technique. *J. Micromech. Microeng.* **2010**, *20*, 075005.
103. Atkin, M.; Poetter, K.; Cattrall, R.; Harvey, E. Microfabricated Polymer Filter Device for Bio-Applications. *Proc. SPIE* **2004**, 138–146.
104. Saxena, I.; Agrawal, A.; Joshi, S. S. Fabrication of Microfilters Using Excimer Laser Micromachining and Testing of Pressure Drop. *J. Micromech. Microeng.* **2009**, *19*, 025025.
105. Whitesides, G. M. The Origins and the Future of Microfluidics. *Nature* **2006**, *442*, 368–373.
106. Toner, M.; Irimia, D. Blood-on-a-Chip. *Annu. Rev. Biomed. Eng.* **2005**, *7*, 77–103.
107. Yeo, L. Y.; Chang, H. C.; Chan, P. P. Y.; Friend, J. R. Microfluidic Devices for Bioapplications. *Small* **2011**, *7*, 12–48.
108. Bhagat, A. A. S.; Bow, H.; Hou, H. W.; Tan, S. J.; Han, J.; Lim, C. T. Microfluidics for Cell Separation. *Med. Biol. Eng. Comput.* **2010**, *48*, 999–1014.
109. van den Berg, A.; Craighead, H. G.; Yang, P. From Microfluidic Applications to Nanofluidic Phenomena. *Chem. Soc. Rev.* **2010**, *39*, 899–900.
110. Hou, H. W.; Bhagat, A. A. S.; Lee, W. C.; Huang, S.; Han, J.; Lim, C. T. Microfluidic Devices for Blood Fractionation. *Micromachines* **2011**, *2*, 319–343.
111. Crowley, T. A.; Pizziconi, V. Isolation of Plasma from Whole Blood Using Planar Microfilters for Lab-on-a-Chip Applications. *Lab Chip* **2005**, *5*, 922–929.
112. Ji, H. M.; Samper, V.; Chen, Y.; Heng, C. K.; Lim, T. M.; Yobas, L. Silicon-Based Microfilters for Whole Blood Cell Separation. *Biomed. Microdevices* **2008**, *10*, 251–257.
113. Wilding, P.; Kricka, L. J.; Cheng, J.; Hvichia, G.; Shoffner, M. A.; Fortina, P. Integrated Cell Isolation and Polymerase Chain Reaction Analysis Using Silicon Microfilter Chambers. *Anal. Biochem.* **1998**, *257*, 95–100.
114. Wilding, P.; Shoffner, M. A.; Kricka, L. J. PCR in a Silicon Microstructure. *Clin. Chem.* **1994**, *40*, 1815–1818.
115. Volkmuth, W.; Austin, R. DNA Electrophoresis in Microlithographic Arrays. *Nature* **1992**, *358*, 600–602.
116. Fu, J.; Yoo, J.; Han, J. Molecular Sieving in Periodic Free-Energy Landscapes Created by Patterned Nanofilter Arrays. *Phys. Rev. Lett.* **2006**, *97*, 18103.
117. Han, J.; Craighead, H. Separation of Long DNA Molecules in a Microfabricated Entropic Trap Array. *Science* **2000**, *288*, 1026–1029.
118. Fu, J.; Mao, P.; Han, J. Nanofilter Array Chip for Fast Gel-Free Biomolecule Separation. *Appl. Phys. Lett.* **2005**, *87*, 263902–263903.
119. Han, J.; Fu, J.; Schoch, R. B. Molecular Sieving Using Nanofilters: Past, Present and Future. *Lab Chip* **2007**, *8*, 23–33.
120. Chaw, K.; Manimaran, M.; Tay, E.; Swaminathan, S. Multi-step Microfluidic Device for Studying Cancer Metastasis. *Lab Chip* **2007**, *7*, 1041–1047.
121. Peh, X.; Zhu, L.; Teo, C.; Ji, H.; Feng, H.; Liu, W. T. Rapid Detection of Waterborne Protozoa in Environmental Samples with a Filter-Based Biochip. *IEEE Solid-State Sens., Actuators Microsyst. Conf.* 2007; pp 1861−1864.
122. Mohamed, H.; Turner, J. N.; Caggana, M. Biochip for Separating Fetal Cells from Maternal Circulation. *J. Chromatogr., A* **2007**, *1162*, 187–192.
123. Panaro, N. J.; Lou, X. J.; Fortina, P.; Kricka, L. J.; Wilding, P. Micropillar Array Chip for Integrated White Blood Cell Isolation and PCR. *Biomol. Eng.* **2005**, *21*, 157–162.
124. Mohamed, H.; Murray, M.; Turner, J. N.; Caggana, M. Isolation of Tumor Cells Using Size and Deformation. *J. Chromatogr., A* **2009**, *1216*, 8289–8295.
125. Murthy, S. K.; Sethu, P.; Vunjak-Novakovic, G.; Toner, M.; Radisic, M. Size-Based Microfluidic Enrichment of Neonatal Rat Cardiac Cell Populations. *Biomed. Microdevices* **2006**, *8*, 231–237.
126. Chen, X.; Cui, D. F.; Liu, C. C.; Li, H. Microfluidic Chip for Blood Cell Separation and Collection Based on Crossflow Filtration. *Sens. Actuators, B* **2008**, *130*, 216–221.
127. Yoon, Y. K.; Park, J. H.; Cros, F.; Allen, M. G. *Integrated Vertical Screen Microfilter System Using Inclined Su-8 Structures*. The Sixteenth Annual International Conference on Micro Electro Mechanical Systems, MEMS 2003, Kyoto, IEEE: Kyoto, Japan, **2003**, pp 227−230.
128. Koros, W.; Ma, Y.; Shimidzu, T. Terminology for Membranes and Membrane Processes (Iupac Recommendations 1996). *J. Membr. Sci.* **1996**, *120*, 149–159.
129. VanDelinder, V.; Groisman, A. Perfusion in Microfluidic Cross-Flow: Separation of White Blood Cells from Whole Blood and Exchange of Medium in a Continuous Flow. *Anal. Chem.* **2007**, *79*, 2023–2030.
130. Lee, D.; Sukumar, P.; Mahyuddin, A.; Choolani, M.; Xu, G. Separation of Model Mixtures of Epsilon-Globin Positive Fetal Nucleated Red Blood Cells and Anucleate Erythrocytes Using a Microfluidic Device. *J. Chromatogr., A* **2010**, *1217*, 1862–1866.
131. Prenen, A. M.; Knopf, A.; Bastiaansen, C. W. M.; Broer, D. J. *In-Situ* Fabrication of Polymer Microsieves for Mtas by Slanted Angle Holography. *Microfluid. Nanofluid.* **2011**, *10*, 1299–1304.
132. Poinern, G. E. J.; Ali, N.; Fawcett, D. Progress in Nano-engineered Anodic Aluminum Oxide Membrane Development. *Materials* **2011**, *4*, 487–526.
133. Jirage, K. B.; Hulteen, J. C.; Martin, C. R. Nanotubule-Based Molecular-Filtration Membranes. *Science* **1997**, *278*, 655–658.
134. Huber, C.; Huber, T.; Sadoqi, M.; Lubin, J.; Manalis, S.; Prater, C. Nanowire Array Composites. *Science* **1994**, *263*, 800–802.
135. Meng, G.; Han, F.; Zhao, X.; Chen, B.; Yang, D.; Liu, J.; Xu, Q.; Kong, M.; Zhu, X.; Jung, Y. J. A General Synthetic Approach to Interconnected Nanowire/Nanotube and Nanotube/Nanowire/Nanotube Heterojunctions with Branched Topology. *Angew. Chem.* **2009**, *121*, 7302–7306.
136. Kim, K.; Kim, M.; Cho, S. M. Pulsed Electrodeposition of Palladium Nanowire Arrays Using AAO Template. *Mater. Chem. Phys.* **2006**, *96*, 278–282.
137. Kyotani, T.; Tsai, L.; Tomita, A. Formation of Ultrafine Carbon Tubes by Using an Anodic Aluminum Oxide Film as a Template. *Chem. Mater.* **1995**, *7*, 1427–1428.
138. Sui, Y.; Gonzalez-Leon, J.; Bermudez, A.; Saniger, J. Synthesis of Multi Branched Carbon Nanotubes in Porous Anodic Aluminum Oxide Template. *Carbon* **2001**, *39*, 1709–1715.
139. Masuda, H.; Satoh, M. Fabrication of Gold Nanodot Array Using Anodic Porous Alumina as an Evaporation Mask. *Jpn. J. Appl. Phys.* **1996**, *35*, L126–L129.
140. Liang, J.; Luo, H.; Beresford, R.; Xu, J. A Growth Pathway for Highly Ordered Quantum Dot Arrays. *Appl. Phys. Lett.* **2004**, *85*, 5974.
141. Akselrod, M. S.; Akselrod, A. E.; Orlov, S. S.; Sanyal, S.; Underwood, T. H. *New Aluminum Oxide Single Crystals for Voltric Optical Data Storage*; Optical Data Storage: Vancouver, BC Canada, 2003.
142. Preston, C. K.; Moskovits, M. Optical Characterization of Anodic Aluminum Oxide Films Containing Electrochemically

Deposited Metal Particles. 1. Gold in Phosphoric Acid Anodic Aluminum Oxide Films. *J. Phys. Chem.* **1993**, *97*, 8495–8503.
143. Masuda, H.; Abe, A.; Nakao, M.; Yokoo, A.; Tamamura, T.; Nishio, K. Ordered Mosaic Nanocomposites in Anodic Porous Alumina. *Adv. Mater.* **2003**, *15*, 161–164.
144. Sander, M. S.; Tan, L. S. Nanoparticle Arrays on Surfaces Fabricated Using Anodic Alumina Films as Templates. *Adv. Funct. Mater.* **2003**, *13*, 393–397.
145. Yamaguchi, A.; Uejo, F.; Yoda, T.; Uchida, T.; Tanamura, Y.; Yamashita, T.; Teramae, N. Self-Assembly of a Silica–Surfactant Nanocomposite in a Porous Alumina Membrane. *Nat. Mater.* **2004**, *3*, 337–341.
146. Penumetcha, S. S.; Kona, R.; Hardin, J. L.; Molder, A. L.; Steinle, E. D. Monitoring Transport across Modified Nanoporous Alumina Membranes. *Sensors* **2007**, *7*, 2942–2952.
147. Gong, D.; Yadavalli, V.; Paulose, M.; Pishko, M.; Grimes, C. A. Controlled Molecular Release Using Nanoporous Alumina Capsules. *Biomed. Microdevices* **2003**, *5*, 75–80.
148. Sadasivan, V.; Richter, C. P.; Menon, L.; Williams, P. F. Electrochemical Self-Assembly of Porous Alumina Templates. *AIChE J.* **2005**, *51*, 649–655.
149. Thompson, G.; Wood, G. Porous Anodic Film Formation on Aluminium. *Nature* **1981**, *290*, 230–232.
150. Thompson, G. Porous Anodic Alumina: Fabrication, Characterization and Applications. *Thin Solid Films* **1997**, *297*, 192–201.
151. Lee, W.; Ji, R.; Gösele, U.; Nielsch, K. Fast Fabrication of Long-Range Ordered Porous Alumina Membranes by Hard Anodization. *Nat. Mater.* **2006**, *5*, 741–747.
152. Lo, D.; Budiman, R. A. Fabrication and Characterization of Porous Anodic Alumina Films from Impure Aluminum Foils. *J. Electrochem. Soc.* **2007**, *154*, C60.
153. Chen, W.; Wu, J. S.; Yuan, J. H.; Xia, X. H.; Lin, X. H. An Environment-Friendly Electrochemical Detachment Method for Porous Anodic Alumina. *J. Electroanal. Chem.* **2007**, *600*, 257–264.
154. Masuda, H.; Yamada, H.; Satoh, M.; Asoh, H.; Nakao, M.; Tamamura, T. Highly Ordered Nanochannel-Array Architecture in Anodic Alumina. *Appl. Phys. Lett.* **1997**, *71*, 2770.
155. Masuda, H.; Fukuda, K. Ordered Metal Nanohole Arrays Made by a Two-Step Replication of Honeycomb Structures of Anodic Alumina. *Science* **1995**, *268*, 1466–1468.
156. Nishio, K.; Nakao, M.; Yokoo, A.; Masuda, H. Ideally Ordered Metal Hole Arrays with High Aspect Ratios Prepared from Anodic Porous Alumina. *Jpn. J. Appl. Phys.* **2003**, *42*, L83–L85.
157. Asoh, H.; Nishio, K.; Nakao, M.; Yokoo, A.; Tamamura, T.; Masuda, H. Fabrication of Ideally Ordered Anodic Porous Alumina with 63 nm Hole Periodicity Using Sulfuric Acid. *J. Vac. Sci. Technol., B* **2001**, *19*, 569–572.
158. Choi, J.; Nielsch, K.; Reiche, M.; Wehrspohn, R.; Gösele, U. Fabrication of Monodomain Alumina Pore Arrays with an Interpore Distance Smaller Than the Lattice Constant of the Imprint Stamp. *J. Vac. Sci. Technol., B* **2003**, *21*, 763.
159. Masuda, H.; Yotsuya, M.; Asano, M.; Nishio, K.; Nakao, M.; Yokoo, A.; Tamamura, T. Self-Repair of Ordered Pattern of Nanometer Dimensions Based on Self-Compensation Properties of Anodic Porous Alumina. *Appl. Phys. Lett.* **2001**, *78*, 826.
160. Liu, C.; Datta, A.; Wang, Y. Ordered Anodic Alumina Nanochannels on Focused-Ion-Beam-Prepatterned Aluminum Surfaces. *Appl. Phys. Lett.* **2001**, *78*, 120.
161. Masuda, H.; Matsui, Y.; Yotsuya, M.; Matsumoto, F.; Nishio, K. Fabrication of Highly Ordered Anodic Porous Alumina Using Self-Organized Polystyrene Particle Array. *Chem. Lett.* **2004**, *33*, 584–585.
162. Matsui, Y.; Nishio, K.; Masuda, H. Highly Ordered Anodic Porous Alumina by Imprinting Using Ni Molds Prepared from Ordered Array of Polystyrene Particles. *Jpn. J. Appl. Phys.* **2005**, *44*, 7726.
163. Yanagishita, T.; Nishio, K.; Masuda, H. Polymer Through-Hole Membranes with High Aspect Ratios from Anodic Porous Alumina Templates. *Jpn. J. Appl. Phys.* **2006**, *45*, L1133–L1135.
164. Furneaux, R.; Rigby, W.; Davidson, A. The Formation of Controlled-Porosity Membranes from Anodically Oxidized Aluminium. *Nature* **1989**, *337*, 147–149.
165. Lei, Y.; Cai, W.; Wilde, G. Highly Ordered Nanostructures with Tunable Size, Shape and Properties: A New Way to Surface Nano-patterning Using Ultra-thin Alumina Masks. *Prog. Mater. Sci.* **2007**, *52*, 465–539.
166. Csokan, P. Some Observations on the Growth Mechanism of Hard Anodic Oxide Coatings on Aluminium. *Trans. Inst. Met. Finish.* **1964**, *41*, 51–56.
167. Müller, F.; Birner, A.; Gösele, U.; Lehmann, V.; Ottow, S.; Föll, H. Structuring of Macroporous Silicon for Applications as Photonic Crystals. *J. Porous Mater.* **2000**, *7*, 201–204.
168. Peng, K. Q.; Wang, X.; Li, L.; Wu, X. L.; Lee, S. T. High-Performance Silicon Nanohole Solar Cells. *J. Am. Chem. Soc.* **2010**, *132*, 6872–6873.
169. Zacharatos, F.; Gianneta, V.; Nassiopoulou, A. G. Highly Ordered Hexagonally Arranged Sub 200 nm Diameter Vertical Cylindrical Pores on p-Type Si Using Non-lithographic Pre-patterning of the Si Substrate. *Phys. Status Solidi A* **2009**, *206*, 1286–1289.
170. Lehmann, V.; Stengl, R.; Reisinger, H.; Detemple, R.; Theiss, W. Optical Shortpass Filters Based on Macroporous Silicon. *Appl. Phys. Lett.* **2001**, *78*, 589.
171. Föll, H.; Christophersen, M.; Carstensen, J.; Hasse, G. Formation and Application of Porous Silicon. *Mater. Sci. Eng., R* **2002**, *39*, 93–141.
172. Sabzi, R. E.; Kant, K.; Losic, D. Electrochemical Synthesis of Nickel Hexacyanoferrate Nanoarrays with Dots, Rods and Nanotubes Morphology Using a Porous Alumina Template. *Electrochim. Acta* **2010**, *55*, 1829–1835.
173. Martin, C. R.; Kohli, P. The Emerging Field of Nanotube Biotechnology. *Nat. Rev. Drug Discovery* **2003**, *2*, 29–37.
174. Lee, S. B.; Mitchell, D. T.; Trofin, L.; Nevanen, T. K.; Söderlund, H.; Martin, C. R. Antibody-Based Bio-Nanotube Membranes for Enantiomeric Drug Separations. *Science* **2002**, *296*, 2198–2200.
175. Buyukserin, F.; Kang, M.; Martin, C. R. Plasma-Etched Nanopore Polymer Films and Their Use as Templates To Prepare "Nano Test Tubes". *Small* **2007**, *3*, 106–110.
176. Wirtz, M.; Parker, M.; Kobayashi, Y.; Martin, C. R. Molecular Sieving and Sensing with Gold Nanotube Membranes. *Chem. Rec.* **2002**, *2*, 259–267.
177. Kumar, N.; Tian, M.; Wang, J.; Watts, W.; Kindt, J.; Mallouk, T.; Chan, M. Investigation of Superconductivity in Electrochemically Fabricated AuSn Nanowires. *Nanotechnology* **2008**, *19*, 365704.
178. Wang, J.; Shi, C.; Tian, M.; Zhang, Q.; Kumar, N.; Jain, J.; Mallouk, T.; Chan, M. Proximity-Induced Superconductivity in Nanowires: Minigap State and Differential Magnetoresistance Oscillations. *Phys. Rev. Lett.* **2009**, *102*, 247003.
179. Hicks, L.; Dresselhaus, M. Effect of Quantum-Well Structures on the Thermoelectric Figure of Merit. *Phys. Rev. B* **1993**, *47*, 12727.
180. He, B.; Son, S. J.; Lee, S. B. Shape-Coded Silica Nanotubes for Biosensing. *Langmuir* **2006**, *22*, 8263–8265.
181. Baik, J. M.; Zielke, M.; Kim, M. H.; Turner, K. L.; Wodtke, A. M.; Moskovits, M. Tin-Oxide-Nanowire-Based Electronic Nose Using Heterogeneous Catalysis as a Functionalization Strategy. *ACS Nano* **2010**, *4*, 3117–3122.
182. Lee, J.; Mubeen, S.; Ji, X.; Stucky, G. D.; Moskovits, M. Plasmonic Photoanodes for Solar Water Splitting with Visible Light. *Nano Lett.* **2012**, *12*, 5014–5019.
183. Dekker, C. Solid-State Nanopores. *Nat. Nanotechnol.* **2007**, *2*, 209–215.
184. Kim, M. J.; Wanunu, M.; Bell, D. C.; Meller, A. Rapid Fabrication of Uniformly Sized Nanopores and Nanopore Arrays for Parallel DNA Analysis. *Adv. Mater.* **2006**, *18*, 3149–3153.
185. Venkatesan, B. M.; Dorvel, B.; Yemenicioglu, S.; Watkins, N.; Petrov, I.; Bashir, R. Highly Sensitive, Mechanically

Stable Nanopore Sensors for DNA Analysis. *Adv. Mater.* **2009**, *21*, 2771–2776.
186. Healy, K. Nanopore-Based Single-Molecule DNA Analysis. *Nanomedicine* **2007**, *2*, 459–481.
187. Soni, G. V.; Meller, A. Progress toward Ultrafast DNA Sequencing Using Solid-State Nanopores. *Clin. Chem.* **2007**, *53*, 1996–2001.
188. Branton, D.; Deamer, D. W.; Marziali, A.; Bayley, H.; Benner, S. A.; Butler, T.; Di Ventra, M.; Garaj, S.; Hibbs, A.; Huang, X. The Potential and Challenges of Nanopore Sequencing. *Nat. Biotechnol.* **2008**, *26*, 1146–1153.
189. Healy, K.; Schiedt, B.; Morrison, A. P. Solid-State Nanopore Technologies for Nanopore-Based DNA Analysis. *Nanomedicine* **2007**, *2*, 875–897.
190. Ivanov, A. P.; Wilson, K. A.; Doğan, F.; Japrung, D.; Edel, J. B. Single Molecule Sensing with Solid-State Nanopores: Novel Materials, Methods, and Applications. *Chem. Soc. Rev.* **2012**, *42*, 15–28.
191. Venkatesan, B. M.; Bashir, R. Nanopore Sensors for Nucleic Acid Analysis. *Nat. Nanotechnol.* **2011**, *6*, 615–624.
192. Li, J.; Stein, D.; McMullan, C.; Branton, D.; Aziz, M. J.; Golovchenko, J. A. Ion-Beam Sculpting at Nanometre Length Scales. *Nature* **2001**, *412*, 166–169.
193. Storm, A.; Chen, J.; Ling, X.; Zandbergen, H.; Dekker, C. Fabrication of Solid-State Nanopores with Single-Nanometre Precision. *Nat. Mater.* **2003**, *2*, 537–540.
194. Chen, P.; Mitsui, T.; Farmer, D. B.; Golovchenko, J.; Gordon, R. G.; Branton, D. Atomic Layer Deposition to Fine-Tune the Surface Properties and Diameters of Fabricated Nanopores. *Nano Lett.* **2004**, *4*, 1333–1337.
195. Wanunu, M.; Meller, A. Chemically Modified Solid-State Nanopores. *Nano Lett.* **2007**, *7*, 1580–1585.
196. Storm, A.; Chen, J.; Zandbergen, H.; Dekker, C. Translocation of Double-Strand DNA through a Silicon Oxide Nanopore. *Phys. Rev. E* **2005**, *71*, 051903.
197. Storm, A. J.; Storm, C.; Chen, J.; Zandbergen, H.; Joanny, J. F.; Dekker, C. Fast DNA Translocation through a Solid-State Nanopore. *Nano Lett.* **2005**, *5*, 1193–1197.
198. Li, J.; Gershow, M.; Stein, D.; Brandin, E.; Golovchenko, J. DNA Molecules and Configurations in a Solid-State Nanopore Microscope. *Nat. Mater.* **2003**, *2*, 611–615.
199. Miles, B. N.; Ivanov, A. P.; Wilson, K. A.; Dogan, F.; Japrung, D.; Edel, J. B. Single Molecule Sensing with Solid-State Nanopores: Novel Materials, Methods, and Applications. *Chem. Soc. Rev.* **2013**, *42*, 15–28.
200. Fologea, D.; Uplinger, J.; Thomas, B.; McNabb, D. S.; Li, J. Slowing DNA Translocation in a Solid-State Nanopore. *Nano Lett.* **2005**, *5*, 1734–1737.
201. Zhang, B.; Galusha, J.; Shiozawa, P. G.; Wang, G.; Bergren, A. J.; Jones, R. M.; White, R. J.; Ervin, E. N.; Cauley, C. C.; White, H. S. Bench-Top Method for Fabricating Glass-Sealed Nanodisk Electrodes, Glass Nanopore Electrodes, and Glass Nanopore Membranes of Controlled Size. *Anal. Chem.* **2007**, *79*, 4778–4787.
202. Lan, W.-J.; Holden, D. A.; Zhang, B.; White, H. S. Nanoparticle Transport in Conical-Shaped Nanopores. *Anal. Chem.* **2011**, *83*, 3840–3847.
203. White, R. J.; Ervin, E. N.; Yang, T.; Chen, X.; Daniel, S.; Cremer, P. S.; White, H. S. Single Ion-Channel Recordings Using Glass Nanopore Membranes. *J. Am. Chem. Soc.* **2007**, *129*, 11766–11775.
204. Vlassiouk, I.; Apel, P. Y.; Dmitriev, S. N.; Healy, K.; Siwy, Z. S. Versatile Ultrathin Nanoporous Silicon Nitride Membranes. *Proc. Natl. Acad. Sci. U.S.A.* **2009**, *106*, 21039–21044.
205. Siwy, Z.; Apel, P.; Baur, D.; Dobrev, D. D.; Korchev, Y. E.; Neumann, R.; Spohr, R.; Trautmann, C.; Voss, K.-O. Preparation of Synthetic Nanopores with Transport Properties Analogous to Biological Channels. *Surf. Sci.* **2003**, *532*, 1061–1066.
206. Mara, A.; Siwy, Z.; Trautmann, C.; Wan, J.; Kamme, F. An Asymmetric Polymer Nanopore for Single Molecule Detection. *Nano Lett.* **2004**, *4*, 497–501.
207. Jackson, E. A.; Hillmyer, M. A. Nanoporous Membranes Derived from Block Copolymers: From Drug Delivery to Water Filtration. *ACS Nano* **2010**, *4*, 3548–3553.
208. Ulbricht, M. Advanced Functional Polymer Membranes. *Polymer* **2006**, *47*, 2217–2262.
209. Wan, L. S.; Li, J. W.; Ke, B. B.; Xu, Z. K. Ordered Microporous Membranes Templated by Breath Figures for Size-Selective Separation. *J. Am. Chem. Soc.* **2012**, *134*, 95–98.
210. Kim, S. H.; Misner, M. J.; Xu, T.; Kimura, M.; Russell, T. P. Highly Oriented and Ordered Arrays from Block Copolymers *via* Solvent Evaporation. *Adv. Mater.* **2004**, *16*, 226–231.
211. Schmidt, K.; Schoberth, H. G.; Ruppel, M.; Zettl, H.; Hänsel, H.; Weiss, T. M.; Urban, V.; Krausch, G.; Böker, A. Reversible Tuning of a Block-Copolymer Nanostructure *via* Electric Fields. *Nat. Mater.* **2007**, *7*, 142–145.
212. Olszowka, V.; Hund, M.; Kuntermann, V.; Scherdel, S.; Tsarkova, L.; Böker, A. Electric Field Alignment of a Block Copolymer Nanopattern: Direct Observation of the Microscopic Mechanism. *ACS Nano* **2009**, *3*, 1091–1096.
213. Hamley, I. Crystallization in Block Copolymers. *Adv. Polym. Sci.* **1999**, *148*, 113–137.
214. Kim, B. S.; Qiu, J. M.; Wang, J. P.; Taton, T. A. Magnetomicelles: Composite Nanostructures from Magnetic Nanoparticles and Cross-Linked Amphiphilic Block Copolymers. *Nano Lett.* **2005**, *5*, 1987–1991.
215. Angelescu, D. E.; Waller, J. H.; Adamson, D. H.; Register, R. A.; Chaikin, P. M. Enhanced Order of Block Copolymer Cylinders in Single-Layer Films Using a Sweeping Solidification Front. *Adv. Mater.* **2007**, *19*, 2687–2690.
216. Hillmyer, M. Nanoporous Materials from Block Copolymer Precursors. *Adv. Polym. Sci.* **2005**, *190*, 137–181.
217. Radano, C. P.; Scherman, O. A.; Stingelin-Stutzmann, N.; Müller, C.; Breiby, D. W.; Smith, P.; Janssen, R. A. J.; Meijer, E. Crystalline-Crystalline Block Copolymers of Regioregular Poly(3-hexylthiophene) and Polyethylene by Ring-Opening Metathesis Polymerization. *J. Am. Chem. Soc.* **2005**, *127*, 12502–12503.
218. Guillet, P.; Fustin, C. A.; Mugemana, C.; Ott, C.; Schubert, U. S.; Gohy, J. F. Tuning Block Copolymer Micelles by Metal−Ligand Interactions. *Soft Matter* **2008**, *4*, 2278–2282.
219. Yang, S. Y.; Ryu, I.; Kim, H. Y.; Kim, J. K.; Jang, S. K.; Russell, T. P. Nanoporous Membranes with Ultrahigh Selectivity and Flux for the Filtration of Viruses. *Adv. Mater.* **2006**, *18*, 709–712.
220. Bang, J.; Jeong, U.; Ryu, D. Y.; Russell, T. P.; Hawker, C. J. Block Copolymer Nanolithography: Translation of Molecular Level Control to Nanoscale Patterns. *Adv. Mater.* **2009**, *21*, 4769–4792.
221. Phillip, W. A.; O'Neill, B.; Rodwogin, M.; Hillmyer, M. A.; Cussler, E. Self-Assembled Block Copolymer Thin Films as Water Filtration Membranes. *ACS Appl. Mater. Interfaces* **2010**, *2*, 847–853.
222. Jeong, B.; Bae, Y. H.; Lee, D. S.; Kim, S. W. Biodegradable Block Copolymers as Injectable Drug-Delivery Systems. *Nature* **1997**, *388*, 860–862.
223. Nunes, S. P.; Behzad, A. R.; Hooghan, B.; Sougrat, R.; Karunakaran, M.; Pradeep, N.; Vainio, U.; Peinemann, K. V. Switchable pH-Responsive Polymeric Membranes Prepared *via* Block Copolymer Micelle Assembly. *ACS Nano* **2011**, *5*, 3516–3522.
224. Olson, D. A.; Chen, L.; Hillmyer, M. A. Templating Nanoporous Polymers with Ordered Block Copolymers. *Chem. Mater.* **2007**, *20*, 869–890.
225. Xu, H.; Goedel, W. A. From Particle-Assisted Wetting to Thin Free-Standing Porous Membranes. *Angew. Chem., Int. Ed.* **2003**, *42*, 4694–4696.
226. Xu, H.; Goedel, W. A. Particle-Assisted Wetting. *Langmuir* **2003**, *19*, 4950–4952.
227. Yan, F.; Ding, A.; Gironès, M.; Lammertink, R. G. H.; Wessling, M.; Börger, L.; Vilsmeier, K.; Goedel, W. A. Microsieves: Hierarchically Structured Assembly of Polymer Microsieves, Made by a Combination of Phase Separation Micromolding

and Float-Casting (Adv. Mater. 12/2012). *Adv. Mater.* **2012**, *24*, 1498–1498.
228. Jahn, S. F.; Engisch, L.; Baumann, R. R.; Ebert, S.; Goedel, W. A. Polymer Microsieves Manufactured by Inkjet Technology. *Langmuir* **2008**, *25*, 606–610.
229. Sears, K.; Dumée, L.; Schütz, J.; She, M.; Huynh, C.; Hawkins, S.; Duke, M.; Gray, S. Recent Developments in Carbon Nanotube Membranes for Water Purification and Gas Separation. *Materials* **2010**, *3*, 127–149.
230. Brady Estévez, A. S.; Kang, S.; Elimelech, M. A Single-Walle-Carbon-Nanotube Filter for Removal of Viral and Bacterial Pathogens. *Small* **2008**, *4*, 481–484.